University of Alberta

Separation of ethylene and ethane by adsorption on titanosilicate

by

Meng Shi

A thesis submitted to the Faculty of Graduate Studies and Research
in partial fulfillment of the requirements for the degree of

Master of Science

in

Chemical Engineering

Chemical & Materials Engineering

Spring 2010
Edmonton, Alberta

Examining Committee

Steven Kuznicki, Chemical and Materials Engineering

Tony Yeung, Chemical and Materials Engineering

Jeffrey Stryker, Chemistry

Dedicated to my parents, Nianhong and Lingfeng

Abstract

The energy costs associated with ethane-ethylene separation could be significantly reduced by the development of alternatives to cryodistillation. This work examined ethylene recovery by equilibrium adsorption on two types of titanosilicate molecular sieve adsorbents, Na-ETS-10 and Zn-RPZ. A practical adsorptive separation of industrial process gas, with a measured binary bed selectivity for ethylene over ethane of approximately 5 at 25°C and 1 atm, was demonstrated using Na-ETS-10 as the adsorbent. The effects of different binder systems and separation flow rates on the mass transfer properties of Na-ETS-10 were examined in order to optimize the separation. High pressure and low temperature, similar to the working conditions in ethylene production plants, were found to increase the separation factor for these materials. Thermal, steam and microwave desorption methods were compared, and microwave desorption was determined to be the most efficient option for ethylene/ethane desorption and Na-ETS-10 regeneration.

Acknowledgements

First and foremost, I would like to thank my supervisor, Dr. Steven Kuznicki, for his guidance, support and kindness. His influence is not only leading me to the world of molecular sieve, but also helping me make my study and life easier during the last two years in Canada. He gives me the opportunity to be successful in the future. My gratitude is also given to the members of my examing committees, Dr. Tony Yeung, Dr. Jeffrey M. Stryker, and Dr. Natalia Semagina, for their criticism and direction.

I would especially like to thank Dr. Amy Dambrowitz, Dr. Christopher C.H. Lin, and Chris Holt, for their assistance with technical writing and manuscript development, also for their countless help in every aspect during my graduate program. Without their help, I can not smoothly graduate.

I sincerely thank Lan Wu, Zhuwei An, Brenda Brindza, Tong Qiu, Chris Street and every members of our research group, from whom I received so much assistance and encouragement over the years.

Special thanks to Dr. Tanya Kuznicki for her assistance with mathematical analysis.

Finally, I am deeply indebted to my parents and my sister, for their love, support and encouragement during my life. Most importantly, send my gratitude to my girlfriend Mianzhen Che, for her love, understanding and patience throughout the years I study in Canada.

Table of Contents

List of Tables

List of Figures

Nomenclature

Abbreviations

CIP	Carbon in pulp
ETS-4	Engelhard titanosilicate-4
ETS-10	Engelhard titanosilicate-10
GAC	Granular activated carbon
GC	Gas chromatography
GIA	Global industry analysts
IGC	Inverse-phase gas chromatography
MEK	Methyl ethyl ketone
OD	Outer diameter
PSA	Pressure swing adsorption
psi	Pound per square inch
RPZ	Reduced pore zorite
TCD	Thermal conductivity detector
TCE	Trichloroethylene
WIPO	World intellectual property organization
ZSM-5	Zeolite socony mobil-5

Notations

A	Surface area
Å	Angstrom
C	Concentration
G	Gibbs free energy
K	Henry's Law constant
K_q	Adsorption equilibrium constant
P	Pressure
R	Gas constant
T	Absolute temperature
V	Volume

W	The volume above the surface
n	Number of moles
wt%	Weight percent

Greek letters

α	Limiting selectivity
ΔG	Free energy change
ΔH	Enthalpy change Heat of adsorption
ΔS	Entropy change
ε	Potential field
μ	Chemical potential
ν	The amount adsorbed at equilibrium
π	Spreading Pressure
θ	Fractional coverage

Chapter 1 Introduction

1.1 Ethylene and ethane separation

Ethylene, containing a carbon-carbon double bond, is the lightest olefinic hydrocarbon. This hydrocarbon has four hydrogen atoms bound to a pair of carbon atoms which are connected by a double bond shown in Figure 1-1. At ambient conditions it is a colorless, flammable gas with a slightly sweet odor.

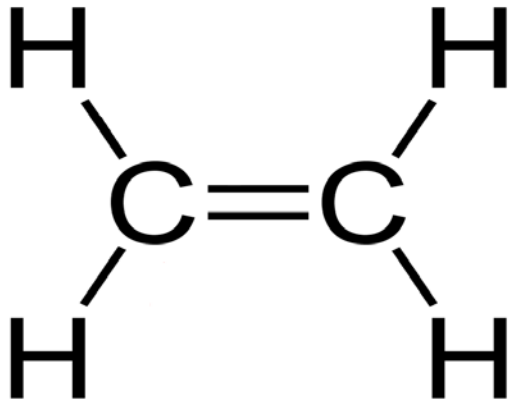

Figure 1-1 Structure of ethylene

The importance of ethylene for the chemical industry is found due to this double bond. Because of the double bond, ethylene is a highly reactive compound which can be converted into a multitude of intermediate and end products on a large industrial scale. Compared with acetylene, it is simpler, safer, and less costly to produce and convert. Ethylene has replaced acetylene as the most important building block in industrial organic chemistry. It can, for example, be used as a ripening hormone for fruit and vegetables. Ethylene acquired its greatest significance, however, as one of the largest volume commodity petrochemicals mostly as a raw material in manufacture of polymers such as polyethylene, polyester, polyvinyl chloride and polystyrene as well as fibers and other organic chemicals. These products are widely used in industrial and consumer

markets including the packaging, transportation and construction industries. According to a new report by Global Industry Analysts, the world ethylene market will reach 160 million tons by 2015 (GIA, 2008). Figure 1-2 presents the comparison of world ethylene capacity breakdown between 1985 and 2010 (Plastemart.com).

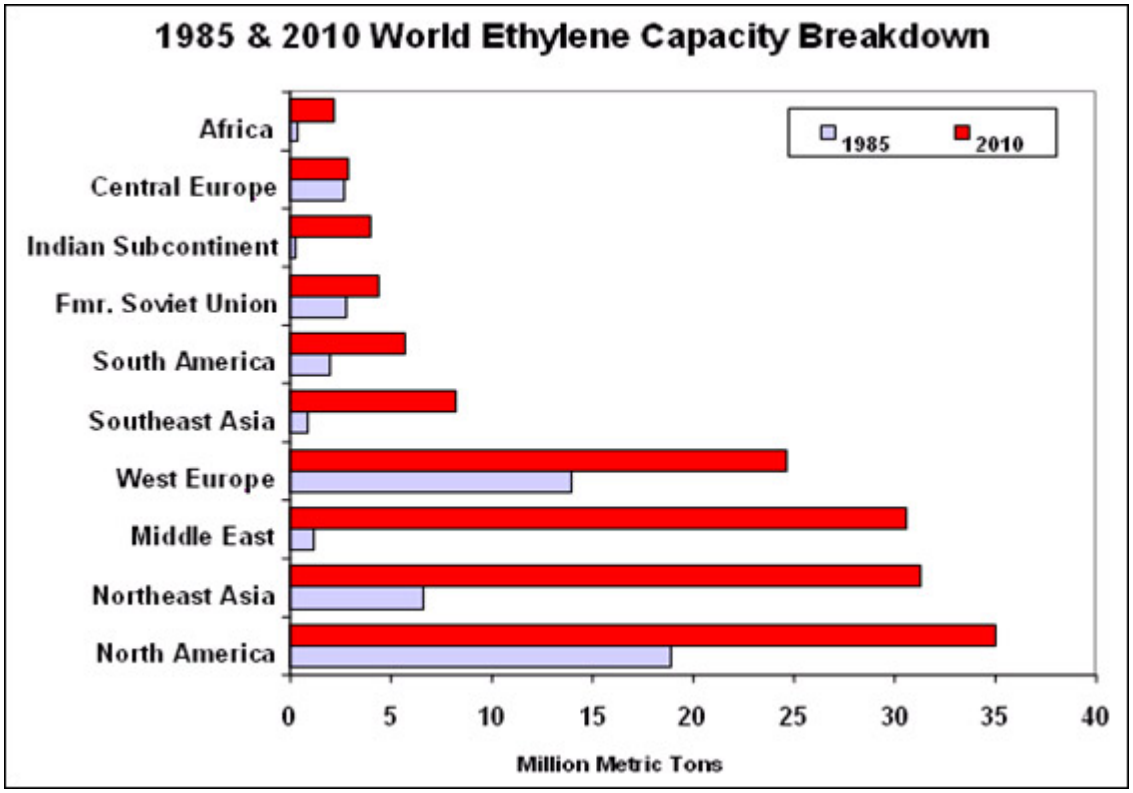

Figure 1-2 1985 & 2010 World Ethylene Capacity Breakdown

Figure 1-3 Ethylene plant in Scholven, Germany

Ethylene is commercially produced by steam cracking and thermal decomposition of a wide range of hydrocarbon feedstocks.

The production of olefins is accomplished by pyrolysis of hydrocarbons in tubular reactor coils installed in externally fired heaters. The cracking of ethane is primarily carried out in the US, Canada and the Middle East by the simple dehydrogenation:

$$C_2H_6 \rightarrow C_2H_4 + H_2$$

In a typical ethylene plant, the cracking represents about 25% of the cost of the unit, while the compression, heating, dehydration, recovery and refrigeration sections represent the remaining percentage of the total (Kniel, 1980). Usually a modern ethylene plants are a complex network with over 300 process engineering assemblies operating at working temperatures from -170°C to well over 1000°C. A typical ethylene plant is

shown in Figure 1-3. This process results in a mixture of ethylene and un-cracked ethane. It is important to purify the ethylene produced in the process and recycle the un-cracked ethane.

Distillation is a method for separating mixtures based on differences in their volatilities in a boiling liquid mixture. When a liquid mixture of two volatile materials is heated, the vapour that comes off will have a higher concentration of the more volatile (lower boiling point) material than the liquid from which it was evolved. Conversely, if a vapour is cooled, the less volatile (higher boiling point) material has a tendency to condense in a greater proportion than the more volatile material. This separation method is widely used in petroleum refineries and petrochemical plants. As the Figure 1-4 illustrated, industrial distillation is typically performed in large, vertical cylindrical columns known as distillation or fractionation towers with diameters ranging from about 65 centimeters to 6 meters and heights ranging from about 6 meters to 60 meters or more. The distillation towers have liquid outlets at intervals along the column which allow for the withdrawal of different fractions or products having different boiling points or boiling ranges. The lightest products (those with the lowest boiling point) exit from the top of the columns and the heaviest products (those with the highest boiling point) exit from the bottom of the column.

Cryogenic distillation has been used in the separation of olefins and paraffins for more than 50 years, although it remains a costly process. Cryogenic distillation processes usually operate near which is usually running around -20°C and 300 psi in a column containing over 100 trays because of the close relative volatilities of the hydrocarbons. This is an energy intensive process which contributes roughly 75% of the overall ethylene

production cost (Kuznicki, S.M., Valerie, A., 2003).

Figure 1-4 A typical distillation tower in industry

Despite the high capital and energy costs associated with cryogenic distillation, this process has remained the dominant technology for light olefin/paraffin separations for many years because of its proven effectiveness and reliability. For example, ethane-ethylene separation (C_2 splitter) is carried out at -25°C and 320 psi in a column containing over 100 trays. The energy costs in olefin/paraffin separations are enormous. The method of olefin/paraffin separation certainly holds an enormous potential for capital and energy cost savings if the ethylene feed is highly enriched.

Several attempts have been made to develop processes with lower energy and equipment costs. Alternative processes include physical adsorption, chemical adsorption, chemical

absorption and membrane separation.

There have been some reports on the use of molecular sieve to separate of C_2H_4/C_2H_6. The molecular sieves chosen for the study were H-mordenite and 13X, CaX, 4A and 5A zeolite by R.W. Triebe (1996). Different ion-exchanged forms of zeolite X were also investigated by H.W. Habgood (1964). The mechanism for chemisorption of ethylene by a metal complex is the ethylene π bond interacts with the σ and π bonds of the metal. Copper and silver ions are commonly used as complexing metals. Ag-exchanged resins have been prepared and studied for C_2H_4/C_2H_6 separation by adsorption at 25°C and 1 atm by Z. Wu (1997). Silver- or Copper- based absorption process also takes advantage of the interaction mechanism presented in chemical adsorption and offers potential for ethylene and ethane separation. A novel solvent system consisting of CuCl/aniline/n-methyl pyrrolidone was evaluated for the reactive absorption of ethylene by T. A. Reine (2005). Various types of polyimide membrane have been developed to separate the ethane and ethylene, and a considerable body of data has been collected relative to membrane permeability and permselectivity (R.L. Burns, 2003). The use of metal-based facilitated transport membranes also have been investigated for C_2H_4/C_2H_6 separation (M. Teramoto, 2005). Continuous process for propylene/propane separation by use of silver nitrate carrier and zirconia porous membrane was also been tested by Chang, J.-W (2002). The mechanism is also based on the forming a reversible complex between ethylene and the metal carrier.

Most of these techniques have disadvantages such as low selectivity, high capital cost and high operating expenses. For example, liquid absorption techniques suffer from solvent loss and need a complex solvent make-up and recovery system.

1.2 Adsorption theory

Adsorptive separation processes are widely used in industry, particularly in the petroleum refining and petrochemical industries.

When a gas is in contact with a solid, part of it is taken up by the solid. The molecules remain on the outside and attach on the surface of the solid. This phenomenon is named adsorption. The solid that takes up the gas is called the adsorbent, and the gas taken up on the surface is called the adsorbate.

Based on the nature of the bonding between the adsorbate molecule and the solid surface, adsorption can happen in two ways, one is physisorption (physical adsorption), the other is chemisorption (chemical adsorption). The bonds formed in physisorption are held by van der Waals and coulombic (or electrostatic) forces, which are very weak, and hence the process is easily reversed. During this process, the chemical identity of the adsorbate remains the same; no change in the covalent structure of the adsorbate takes place. As a spontaneous thermodynamic process, physical adsorption has a negative ΔG. Due to translational degrees of freedom of the gas phase, adsorbate moleculars are lost upon deposition onto the substrate, so ΔS is negative for the physical adsorption. Based on $\Delta G=\Delta H-T\Delta S$, ΔH for this process must be negative, which is exothermic. Chemisorption involves electron transfer and forms a chemical bond between the adsorbate and the solid surface, which is essentially a two-dimensional chemical reaction. This interaction is much stronger than physisorption (S. Brunauer, 1943).

In any adsorption process, an equilibrium is established between the molecules in the gas phase and the corresponding adsorbed phase which are bound to the surface of the solid. For a given gas-solid pair, the amount of gas adsorbed at equilibrium is described by:

$$\nu = f(P,T)$$

where the volume of gas adsorbed ν can be expressed in mL/g under standard conditons. At a fixed temperature, ν is a function of Pressure, and that function is called adsorption isotherm.

Many theories and models have been developed to interpret different types of isotherms. The Langmuir isotherm remains the simplest and most useful model, the Langmuir model is based on these assumptions (Yang, 1997):

- The adsorption system is in dynamic equilibrium, where the rate of evaporation is equal to that of condensation.
- The adsorbed phase molecule is on definite and localized sites.
- Each site can only have one molecule.
- There is no interaction between neighboring adsorbates.

The Langmuir isotherm is derived from equilibrium consideration based on the concept of dynamic equilibrium between the rates of condensation (adsorption) and evaporation (desorption).

To derive the Langmuir isotherm, we can build the following model:

q = molecule * = adsorption site q* = adsorbed molecule

In adsorption, we can have

$$q + * \xrightarrow{k_a} q*$$

The rate of adsorption can be expressed as:

$$r_{ads} = k_a[q][*]$$

In desorption, we can have

$$q* \xrightarrow{k_d} q + *$$

The rate of desorption can be expressed as:

$$r_{des} = k_d[q*]$$

At dynamic equilibrium,

$$k_a[q][*] = k_d[q*]$$

$$\frac{[*]}{[q*]} = \frac{k_d}{k_a[q]} = \frac{1}{K[q]} \quad \frac{[*]}{[q*]} = \frac{k_d}{k_a[q]} = \frac{1}{K[q]}$$

Which,

$$K = \frac{k_a}{k_d}.$$

Consider the total amount of adsorption sites,

$$q^{sat} = [q*] + [*]$$

$$\theta_q = \frac{[q*]}{q^{sat}} = \frac{[q*]}{[q*]+[*]} = \frac{1}{1+\frac{[*]}{[q*]}} = \frac{1}{1+\frac{1}{K[q]}} = \frac{K[q]}{K[q]+1}$$

θ is the coverage or load factor or adsorption capacity.

For ideal gas, we can have $PV = nRT$,

$$C = \frac{n}{V} = \frac{P}{RT}$$

C is concentration.

Combining above two equations,

$$\theta_q = \frac{K_q P_q}{1 + K_q P_q}$$

where K_q is the adsorption equilibrium constant,

When $K_q P_q \to 0$, there is a linear relationship between the coverage and the pressure, which exactly match with Henry's Law,

$$\lim_{p \to 0} \theta_q = K_q P_q$$

K_q is the Henry constant.

When $K_q P_q \to \infty$, $\theta_q \to 1$ which means the surface is completely covered.

The Arrhenius equation gives:

$$k_a = k_{a0} e^{(\frac{-E_{ads}}{RT})}$$

$$k_d = k_{d0} e^{(\frac{-E_{des}}{RT})}$$

$$K = \frac{k_a}{k_d} = \frac{k_{a0}}{k_{b0}} e^{\frac{-(E_{ads} - E_{des})}{RT}} = K_0 e^{\frac{-\Delta H}{RT}}$$

we can obtain:

$$(\frac{\partial \ln K}{\partial T}) = \frac{\Delta H_{ads}}{RT^2}$$

Given a fixed pressure, the extent of the adsorption is determined by the adsorption equilibrium constant *K*, which is in turn dependent on both the temperature *T* and heat of adsorption ΔH_{ads}. The heat of adsorption reflects the strength of the binding of the adsorbent and adsorbate.

The Henry's law constants (K) can be determined directly from the linear region of the isotherms, and can also be calculated from the Langmuir equation applied to low pressure adsorption data. Both methods for the determination of the Henry's law constants give equivalent results. In a binary system, the limiting selectivity (α) of the adsorbent for the

gas A over the gas B is calculated as the ratio of their respective Henry's law constants:

$$\alpha(A/B) = \frac{K_A}{K_B}$$

In a two component mixture, the relative selectivity or separation factor can also be derived from the equilibrium gas phase composition versus the composition of the adsorbed phase, which was illustrated by the equation:

$$\alpha_X^Y = \frac{Y_a \cdot X_g}{Y_g \cdot X_a}$$

Where X_a and Y_a are the mole fractions of the two adsorbates, X and Y, in the adsorbed phase and X_g and Y_g in the gas phase.

In a binary system, based on the information from the inverse-phase gas chromatography (as illustrated in Figure 1-5), we can also calculate the selectivity for the binary system by the equation:

$$\alpha_B^A = \frac{t_2 - t_0}{t_1 - t_0}$$

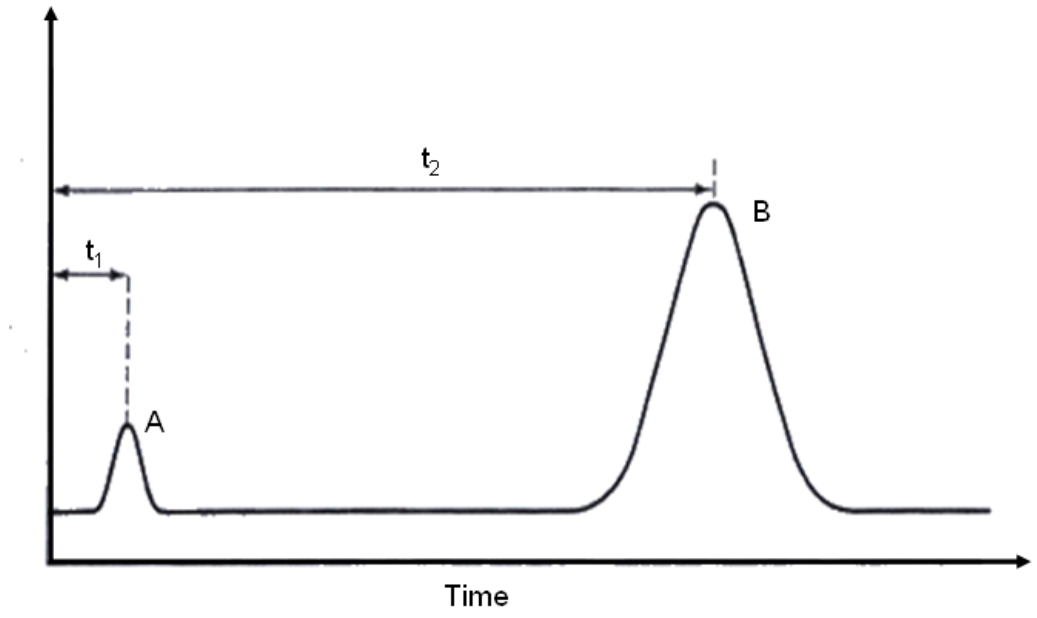

Figure 1-5 An inverse-phase gas chromatography sample for a binary system

Where t_2 is the retention time of the gas B, t_1 is the retention time of gas A, and t_0 is the dead time.

1.3 Zeolite molecular sieves

Commercial adsorbents which exhibit ultraporosity and which are generally used for the separation of gas and vapor mixtures include activated carbons, activated clays, inorganic gels such as silica gel and activated alumina, and the crystalline aluminosilicate zeolites. Table 1-1 presents the applications and annual productions of major industrial sorbents (Yang, 1987).

Table 1-1 Applications and annual productions of major industrial sorbents

Sorbent	*Annual U.S. Production*[a]	*Major Uses for Gas Sorption*
Activated carbon	90,000 (major)	Removal of nonpolar gases and organic vapors (e.g., solvents, gasoline vapor, odors, toxic and radioactive gases); H_2 purification; etc.
Zeolites:		
Synthetic	30,000[b] (major)	Drying; H_2 purification; air purification; air separation; separations based on molecular size and shape (e.g., *n*- and iso-paraffins, aromatics, etc.); gas chromatography
Natural	250,000[b] (minor)	
Silica gel	150,000 (minor)	Drying; gas chromatography
Activated alumina	25,000 (major)	Drying; gas chromatography

[a]Late 1970s figure in metric tons. The fraction used as sorbent is indicated in parentheses.
[b]Worldwide total figure.

Activated carbons, activated alumina, and silica gel do not possess an ordered crystal structure and consequently the pores are non-uniform. The distribution of the pore diameters in the adsorbent particles may be narrow (20-50 Å) or it may range widely as is the case for some activated carbons. Hence, all molecular species, with the possible exception of high molecular weight polymeric materials, may enter the pores. Zeolite molecular sieves have pores of uniform size (3-10 Å) which are uniquely determined by the unit structure of the crystal. These pores will completely exclude molecules which are larger than their diameter. Figure1-6 (Breck, 1974) illustrated the distribution of pore sizes in microporous adsorbents: zeolite A, typical silica gel and activated carbon.

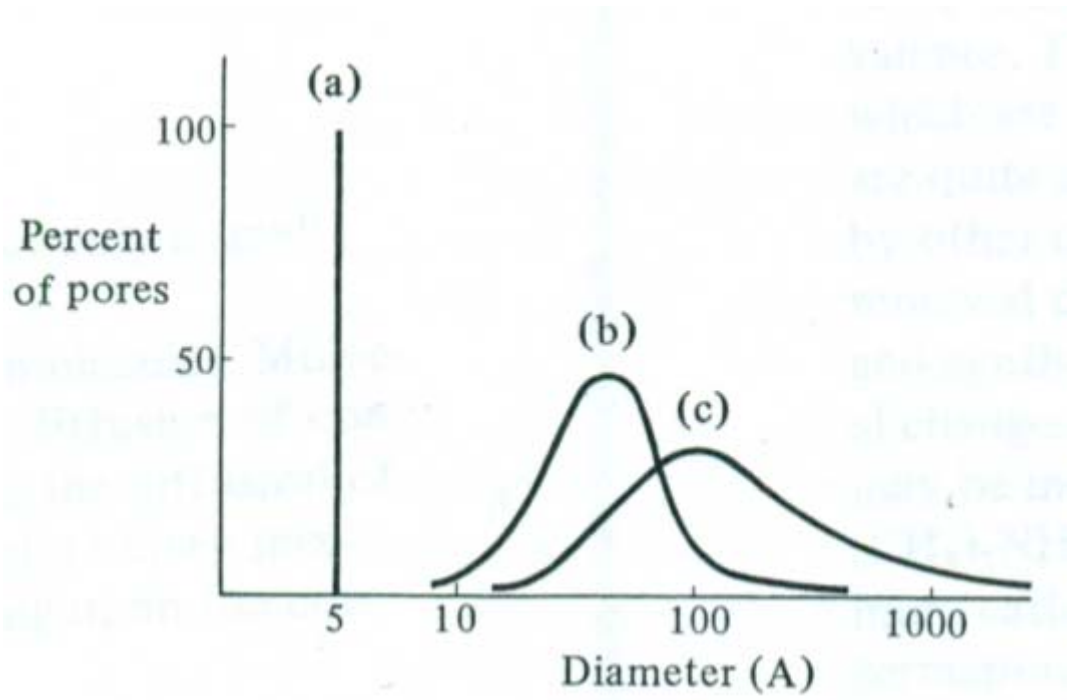

Figure 1-6 Distribution of pore sizes in microporous adsorbents. (a) Zeolite A; (b) typical silica gel; (c) activated carbon (Breck, 1974)

Zeolites are microporous, aluminosilicate minerals, having the general formula (Breck, 1974):

$$x[(M^{I}, M^{II}{}_{1/2}) \cdot AlO_2] \cdot ySiO_2 \cdot zH_2O$$

Where M^{I} = *Li, Na, K, etc.* and M^{II} =*Mg, Ca, Sr, Ba, etc.*

In 1756, a Swedish mineralogist Axel Fredrik Cronstedt discovered that after heating the material stilbite, it produced a large amount of steam from the water that had been adsorbed by the stilbite. Based on this phenomenon, he gave the material the name "zeolite", in Greek, it means "boil stone" (Cronstedt, 1756). There is another name for zeolite, molecular sieve, referring to the unique property of these materials. For example, the ability to selectively sort molecules primarily based on size exclusion. The term was originated by J.W. McBain to define porous solid materials which exhibit the property of acting as sieves on a molecular scale. Initially, most zeolites were natural minerals.

Natural zeolites usually form under the condition that volcanic rocks and ash layers react with alkaline groundwater, also in post-depositional environments over thousands to millions of years in shallow marine basins. Naturally formed zeolites are easily contaminated by the other minerals, metals, and quartz. Because of this, natural zeolites are not candidates for many important commercial applications where uniformity and purity requirements are strict. The history of man-made zeolites can be traced back to the work of Richard Barrer and Robert Milton, commencing in the late 1940s (Vaughan, 1978). Following the foundation built in that period, there has subsequently been a great rise in the number of known synthetic zeolites and also the discovery of new families of zeolite-like or zeolite-related materials, for instance, alumino- and gallo-phosphates, and titanosilicates.

Molecular sieve zeolites were first commercially introduced at 1954 as adsorbents for industrial separations and purifications. Since then the fascination with and the elegance of, this unique class of materials has widely served and contributed most of the major aspect of our lives. They form the heart of hundreds of processes as catalysts, adsorbents, ion-exchange and purification agents, including petroleum cracking for gasoline production, oxygen production from air, and water purification by removing heavy metals. A zeolite is a crystalline aluminosilicate with a three-dimensional framework structure that forms uniformly sized pores of molecular dimensions. As the pores preferentially adsorb molecules that fit snugly inside the pores and exclude molecules that are too large, they act as sieves on a molecular scale. The structure is formed by tetrahedras of (AlO_4) and (SiO_4). These tetrahedras are the basic building blocks for various zeolite structures. Then the framework carries a negative charge. Loosely held cations that sit in the cavities

preserve the electroneutrality of the zeolite. Some of those cations are amenable to cation exchange, and zeolites are able to reversibly adsorb polar molecules (Breck, 1974). A zeolite framework was illustrated by Figure 1-7.

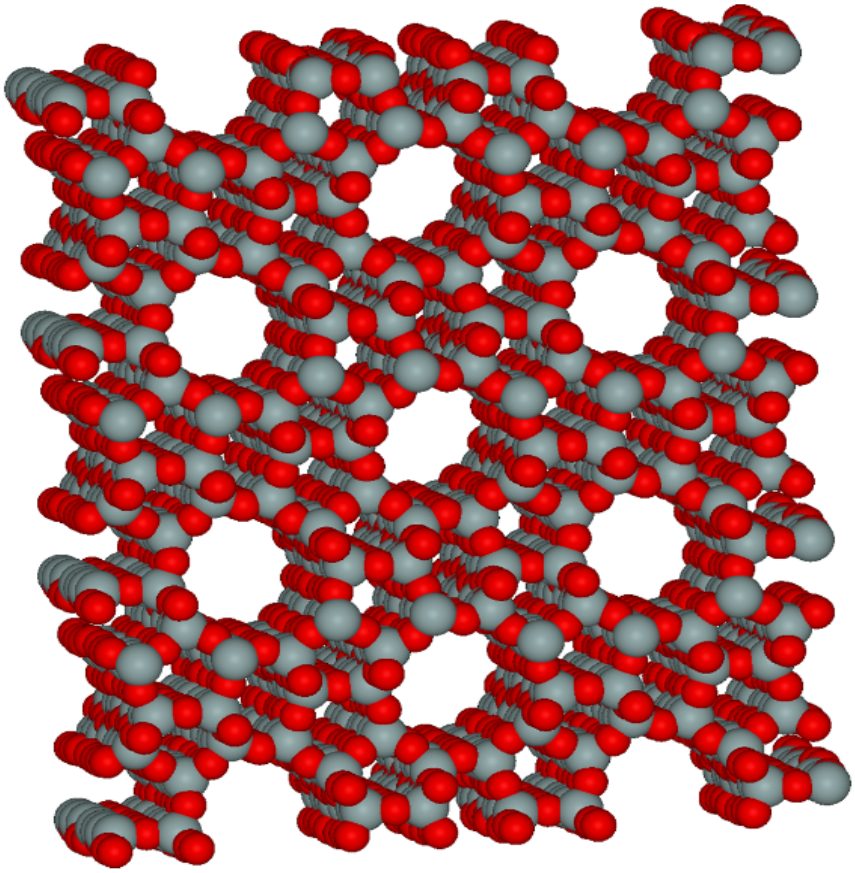

Figure 1-7 A typical zeolite framework

Based on the unique properties of molecular sieves, including crystalline structure, uniform pores, high surface area, and a negatively charged framework with exchangeable cations for charge balance, after hundreds of years of development there are three main applications for molecular sieve zeolites: adsorption, ion-exchange and catalysts.

Table 1-2 Commercial adsorbent applications of molecular sieve zeolites

Applications	Adsorbents
1. Rare gas from Air	ETS-10
2. Drying (Natural Gas)	Zeolite 3A
3. CO_2 removal	Zeolite 5A
4. Sulfur Compound Removal	Cerium-loaded Y-zeolites
5. O_2/N_2 from Air	4A, 5A zeolite
6. Olefin/Paraffin separation	ETS-10

Molecular sieve zeolite adsorbents have been widely applied in separations and purifications in the chemical process industries. A summary list of major adsorbent applications is shown in Table 1-2. The applications can be divided into two categories: purification which is based on surface selectivity for polar or polarizable molecules such as H_2O, CO_2 or sulfur compounds, and the bulk separations which depend on molecular sieving principles.

With the recognition of the acidic properties of hydrogen, multivalent metal cation, and decationized forms of zeolites X and Y, and the novel shape selective properties of

zeolites A, molecular sieve zeolites began to be used in hydrocarbon catalysis. The first main commercial catalytic application was widely used from the catalytic cracking of crude to produce liquid fuels in 1962 (Plank, 1964). A summary of the applications of molecular sieve zeolites in catalysis is shown in Table 1-3. These applications are based on the unique properties of zeolites catalysts which include extremely high strength acid sites, and selectivities related to strong adsorptive forces within the zeolite. In addition to the above properties, zeolites can also been used as shape selective catalysts, which were widely commercialized.

Table 1-3 Commercial catalysis applications of molecular sieve zeolites

Applications	Catalysts
1. Hydrocarbon conversion	Aluminum phosphate
2. Hydrogenation & Dehydrogenation	ZSM-5
3. Hydrodealkylation	Mordenite
4. Methanation	Zeolite Y
5. Shape-selective reforming	ZSM-5
6. Dehydration	NaX zeolite

Since Eichorn first showed that the natural zeolite chabazite and natrolite have the capacity for reversible cation exchange in 1858 (Eichorn, 1858), the phenomenon of ion exchange is one of the most important properties of zeolites to be studied scientifically. The cation exchange properties of traditional aluminosilicate zeolites arise from the isomorphous positioning of aluminium in tetrahedral coordination within the Si/Al

framework. This imposes a net negative charge on the framework ($Si^{4+} \rightarrow Al^{3+}$) counterbalanced by cations held within the cavities and channels. Because of this property, zeolites are widely used as water softening agent in detergents, as well as in wastewater treatment (including industrial, agricultural and radioactive) and animal food supplementation (to regulate ammonia or ammonium levels in the stomach). Ion exchange can also be applied in the modification of pore size of molecular sieves. Furthermore, ion exchange zeolite is used in nanometal fabrication (Kuznicki, 2007). The commercial applications are summarized in Table 1-4.

Table 1-4 Commercial ion exchange applications of molecular sieve zeolites

Applications	Ion-exchangers
1. Detergents	Sodium zeolite A
2. Treatment of radioactive waste	Clinoptilolite
3. Ammonia removal from waste water	Clinoptilolite
4. Regulate ammonium levels in stomach	Natural Zeolite
5. Modification of pore size of the molecular sieve	ETS-4

The three major classes of molecular sieve based adsorptive separations that will be discussed in this work are thermodynamic equilibrium, size exclusion and kinetic separations.

Thermodynamic equilibrium effect: Selectivity results from differences in adsorption strengths and is equilibrium driven. The controlling factors of the adsorption are

adsorbate polarizability and the charge and exposure of sieve sites. For example, the mechanism of ethylene and ethane separation based on titanosilicate ETS-10 is thermodynamic equilibrium. Because the the pore size of ETS-10 has an average kinetic diameter of ~8 Å, which is larger than the molecular diameters of both C_2H_4 and C_2H_6 (4.163 Å and 4.443 Å, respectively) (Sircar and Myers, 2003), these data imply that the mechanism for ethylene/ethane separation on Na-ETS-10 is equilibrium competitive adsorption.

Size exclusion which is also expressed as steric effect: The selectivity of molecular exclusion (steric separation) results from differences in molecular/pore size and can be quasi-equilibrium. The steric effect derives from the molecular sieving property of zeolites. In this case only small and properly shaped molecules can diffuse into the adsorbent, whereas other molecules are completely exlcluded. Steric separation is unique to zeolites because of the uniform aperture size in the crystalline structure. For example, the barium-exchanged titanosilicate ETS-4 with an average pore size of 3-5 Å effectively separates nitrogen (about 3.6 Å) from methane (about 3.8 Å) (US Patent 5989316, 1999).

Kinetic effect: Kinetic separation results from differences in adsorption rates and transition. One of the most important examples is carbon molecular sieve, which has a distribution of pore size, as shown in Figure 1-6. This kind of distribution of pores allows different gases to diffuse at different rates while totally avoiding exclusion of any gases in the mixture. Kinetic separation is used commercially for nitrogen generation from air. The separation is believed to be achieved as a result of a slight difference in the kinetic diameters of nitrogen and oxygen, which results in a relatively high diffusivity for oxygen.

1.4 Titanosilicate molecular sieves for the separation of ethane and ethylene

With slow progress in the discovery of new wide pored aluminosilicate based molecular sieves, researchers have taken various approaches to replace aluminum or silicon in zeolite synthesis in the hope of generating either new zeolite-like framework structures or inducing the formation of qualitatively different active sites than are available in analogous aluminosilicate based materials. A naturally occurring alkaline titanosilicate, identified as "Zorite", was discovered in trace quantities on the Siberian Tundra in 1972 (Mer'kov, 1973) and has been used as a model for the creation of novel synthetic zeolites. U.S. Patent No. 4,853,202, entitled "Large-Pored Crystalline Titanium Molecular Sieve Zeolites" (Kuznicki, 1989), U.S. Patent No. 4,938,939, entitled "Preparation of Small-pored Crystalline Titanium Molecular Sieve Zeolites" (Kuznicki, 1990) and WIPO Patent Application WO/2008/002463, entitled "Titanium Silicate Materials, Method for Their Manufacture, and Method for using such titanium silicate materials for adsorptive fluid separations" (Kuznicki, 2008) describe these synthetic titanium silicates, which can be identified in terms of mole ratios of oxides as follows:

$$1.0 \pm 0.25\ M_{2/n}O:TiO_2:ySiO_2:zH_2O$$

Wherein M is at least one cation having a valence of n, y is from 1.0 to 10.0, and z is from 0 to 100. In a preferred embodiment, M is a mixture of alkali metal cations, particularly sodium and potassium, and y is at least 2.5 and ranges up to about 5.

Engelhard Titanosilicate-10 (ETS-10), which is described in U.S. Patent 4,853,202, is a large-pored, mixed octahedral/ tetrahedral titanium silicate molecular sieve possessing a three-dimensional network of interconnecting channels. Figure 1-8 shows the framework

of the ETS-10 (Anderson, 1994).

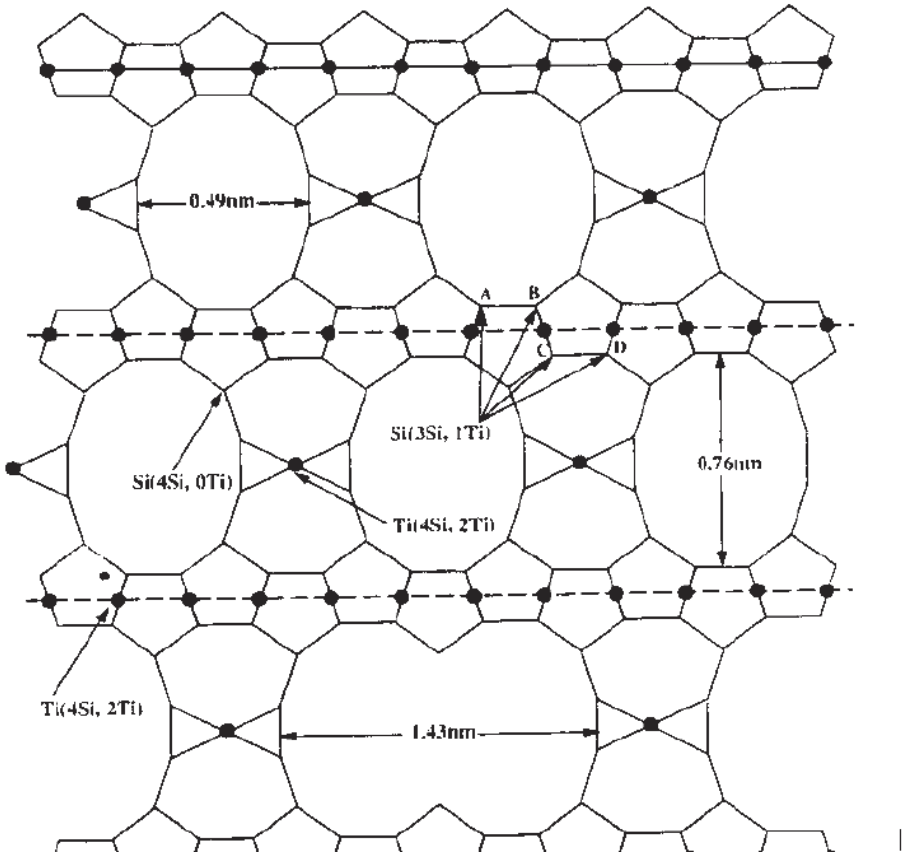

Figure 1-8 Framework of Na-ETS-10

Modelling predictions for the binary adsorption of ethylene and ethane on Na-ETS-10 suggest that this molecular sieve might be an excellent adsorbent for ethylene/ethane separations (Al-Baghli et al., 2006). Recent work investigating the adsorption of ethane and ethylene on the surface of ETS-10 confirms this prediction (Anson et al., 2008; Kuznicki et al, 2009). It should be noted that the pore size of ETS-10 has an average kinetic diameter of ~8 Å, which is larger than the molecular diameters of both C_2H_4 and

C_2H_6 (4.163 Å and 4.443 Å, respectively) (Sircar and Myers, 2003), implying that the mechanism for ethylene/ethane separation on Na-ETS-10 is equilibrium competitive adsorption.

Alternately, size-selective adsorptive separation of C_2H_4 and C_2H_6 could be performed using RPZ (reduced pore zorite), an analog of both ETS-4 (A small-pored, synthetic analogs of the mineral zorite. It is a titanosilicate molecular sieve with an average pore size of 0.3-0.5nm) and mineral zorite. The pore size of RPZ is controlled by the level of structural chloride ions. Chloride ions progressively and systematically constrict the RPZ pore size as their concentration increases, enabling the preparation of thermally stable, size-selective materials (Kuznicki, 2008). The isotherm profiles and adsorption strength of RPZ for selected gases can be modified by ion-exchange of the extra-framework cations. The RPZ adsorbents may also be candidates for the separation of ethane and ethylene by the steric effect.

In this work, inverse-phase gas chromatography (IGC) and low pressure equilibrium adsorption isotherms were measured for C_2H_4 and C_2H_6 on both of these two adsorbents. Separation of the two hydrocarbons was investigated further by constructing a lab-scale demonstration unit. Real process gas from industry was used to test the separation factor, breakthrough profile and capacity for these materials and the two candidates were compared. Different binder and different flow rates were compared and tested, and their adsorption properties were evaluated under high pressure and low temperature. Steam and microwave approaches were tested in the desorption stage to compare with the traditional thermal desorption.

Chapter 2 C_2H_4/C_2H_6 separation by titanosilicate molecular sieves

2.1 Introduction

Since the structure of synthetic titanosilicate was first reported (Kuznicki, 1989), several olefin separations based on different forms of titanosilicate have been investigated. Separation of ethylene from ethane is achieved by feeding a mixture of C_2 hydrocarbons in contact with a crystalline titanium silicate molecular sieve, which has a controlled pore size to selectively adsorb ethylene and size exclude ethane (Kuznicki and Valerie, 2003). Modelling predictions for the binary adsorption of ethylene and ethane on titanosilicate ETS-10 suggest that this molecular sieve might be an excellent adsorbent for ethylene/ethane separations (Al-Baghli and Loughlin, 2006). It should be noted that the pore size of ETS-10 has an average kinetic diameter of ~8 Å, which is larger than the molecular diameters of both C_2H_4 and C_2H_6 (4.163 Å and 4.443 Å, respectively) (Sircar and Myers, 2003). This implies that the mechanism for ethylene/ethane separation on Na-ETS-10 is equilibrium competitive adsorption. ETS-4, with an average pore size of 0.3–0.5 nm, has been applied to multiple separations of mixtures of similar-sized gases, including oxygen/argon, nitrogen/methane, and methane/ethane (Kuznicki, 1990; Kuznicki et al., 1999,2000,2001; Kuznicki and Bell, 2003). RPZ (reduced pore zorite), an analog of both ETS-4 and the mineral zorite, was believed to have the potential to separate ethylene and ethane by the steric effect. Different binder systems and flow rates can affect the adsorption properties of molecular sieve adsorbents, so in addition to selecting an ideal adsorbent, the binder and separation conditions must also be optimized.

2.2 Experimental

ETS-10 was synthesized hydrothermally as reported by Kuznicki (Kuznick, 1991). A typical sample preparation involved thoroughly mixing 50 g of sodium silicate (28.8% SiO_2, 9.14% Na_2O, Fisher), 3.2 g of sodium hydroxide (97+% NaOH, Fisher), 3.8 g of KF (anhydrous, Fisher), 4 g of HCl (1M), and 16.3 g of $TiCl_3$ solution (Fisher). The mixture was stirred in a blender for 1 h, and then reacted in a 125 mL sealed autoclave (PARR Instruments) at 215°C for 64 h. The resultant material was thoroughly washed with de-ionized water, and dried in an oven at 100°C.

A typical sample of RPZ titanosilicate was prepared by mixing 25.1 g of sodium silicate (28.8% SiO_2, 9.14%Na_2O, Fisher), 4.6 g of sodium hydroxide (97% NaOH, Fisher), 3.0 g of KCl (anhydrous,Fisher), and 16.3 g of $TiCl_3$ solution (Fisher). The mixture was stirred in a blender for 1h, and then reacted in a 125 mL sealed autoclave (PARR Instruments) at 200°C for 48 h. The resultant material was washed with de-ionized water, and dried in an oven at 100°C. Zinc ion-exchange was performed by exposing the as-synthesized molecular sieves (as <150 μm powders) to an excess of aqueous ionic solution ($ZnCl_2$) at 100°C with stirring for 24 h. Fully exchanged materials were washed with de-ionized water and dried in an oven at 100°C.

The Na-ETS-10 (Zn-RPZ) materials were pelletized by mixing 6.00 g of the molecular sieves (equilibrated at 100°C) with 2.50 g of Ludox HS-40 colloidal silica (Aldrich). The mixture was homogenized using a mortar and pestle and compressed in a pellet press to 10 000 psi for 3 minutes. The resulting cakes were crushed and sieved to obtain 20-50 mesh particles.

Low pressure equilibrium adsorption isotherms (up to 200 kPa) for ethylene and ethane

on crystalline adsorbent powders were measured volumetrically at 25°C using an AUTOSORB-1-MP from Quantachrome Instruments (Boynton Beach, FL). No binders or diluents were added to the adsorbent samples. Na-ETS-10 was activated at 150°C for 10 h under vacuum (<0.0005 Torr). Zn-RPZ was activated at 200°C for 10 h under vacuum (<0.0005 Torr).

Inverse-phase gas chromatography (IGC) analysis was performed on a Varian 3800 GC equipped with a thermal conductivity detector (TCD). Test adsorbents were packed into 10 inch long copper columns with an OD of 0.25 inch. The columns were filled with 3.5 g of pelletized adsorbents (20-50 mesh). Na-ETS-10 was activated at 150°C for 10 h under a helium flow of 30 mL/min, and Zn-RPZ was activated at 200°C for 10h under a helium flow of 30 mL/min. Characterization gas (pure C_2H_4, pure C_2H_6, and a mixture of 59% C_2H_4 and 41% C_2H_6) was introduced by a 1mL pulse injection into the column. This technique is a useful screening tool for determining the separation characteristics of adsorbents. Single components were injected through the column to measure the elution time of each component gas from the column. These individual experiments were then used to assign the order of gas elution in a mixture of two or more gases.

A scale-up adsorption test was run in an apparatus described in the Figure 2-1. A 50 mL double ended chamber was filled with ～30 g of the pelletized adsorbents (20-50 mesh), which were activated at 150°C for 10 h under a helium flow of 30 cm^3/min for Na-ETS-10, and at 200°C for 10 h for Zn-RPZ. The mixture of 59% C_2H_4 and 41% C_2H_6 was used as the feed gas and the flow rate was adjusted to 180 mL/min. A sampling valve is placed at the outlet of the column for gas collection (used for continuous flow compositional analysis). The outlet gas samples were taken by a 5 mL syringe at 0.5 min or 1 min

increments and analyzed on a modified Varian 3800 GC equipped with a Supelco matrix HayeSep R column for hydrocarbon analysis.

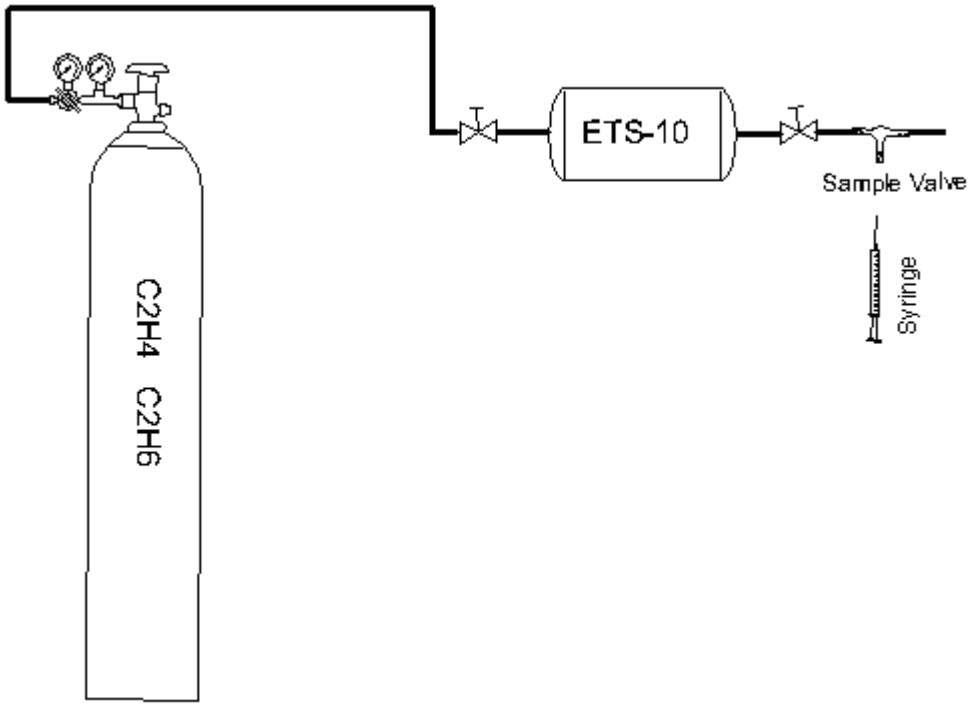

Figure 2-1 Experimental schematic of the gas saturation process

After the process has reached saturation, reflected by the composition of the sample collected at the sample valve (the composition reaches the same as the feed gas), this implies that the system has reached equilibrium. To analysis the composition of the adsorbed phase gases, we directly injected 10 mL pure water into the chamber shown in Figure 2-2, then the adsorbed gases (which should be mixture of ethylene and ethane) were desorbed by the water and collected by the flask. Because ethane and ethylene are difficult dissolve in the water, the gas replaced the water in the flask, and the displaced

water was pushed out and collected by the graduated cylinder. After completely desorption, collected the desorbed gas and analyzed the composition by the IGC analysis.

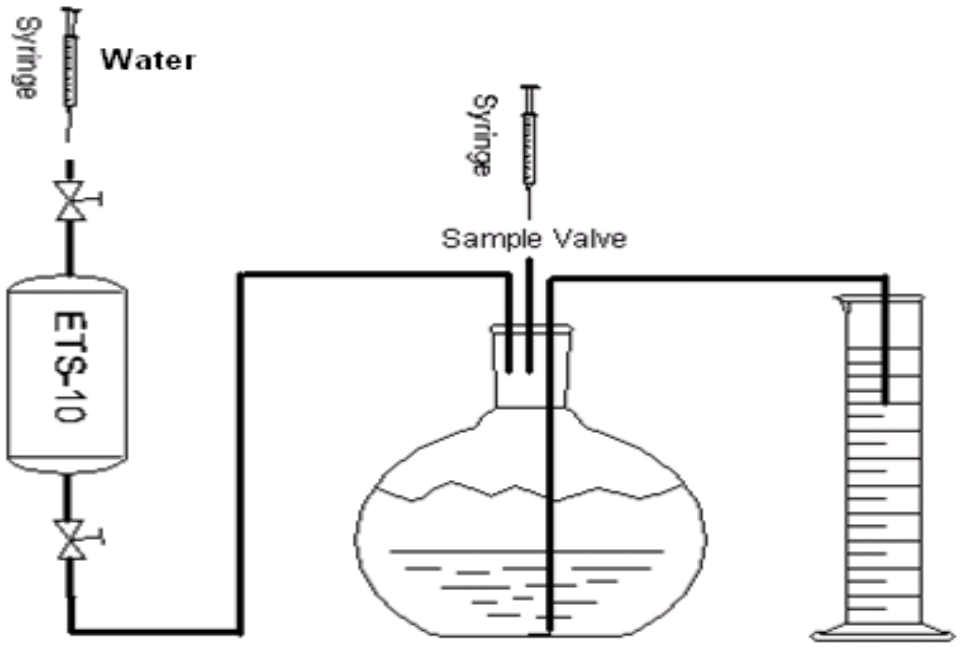

Figure 2-2 Experimental schematic of water desorption process

To demonstrate the impact of flow rate on adsorption and the ethane/ethylene breakthrough profile, different flow rates of the feed gas were investigated.

Flow rates of 400 mL/min, 250 mL/min, 180 mL/min and 115 mL/min were tested. Table 2-1 shows the tests conducted at different flow rates while using pure colloidal silicate (Ludox) as the binder.

Table 2-1 Experiment design for different flow rate investigation

Test No.	Flow rate	Binder
1	400 mL/min	15wt% Ludox
2	250 mL/min	15wt% Ludox
3	180 mL/min	15wt% Ludox
4	115 mL/min	15wt% Ludox

To improve mass transfer properties, we experimented with different binder systems, in conjunction with controlling the gas flow rates. We utilized binders such as pure sodium silicate (NB), pure colloidal silicate (Ludox), actapulgite (actigel), and combinations thereof. The pellets were made as same as described in IGC test section. Table 2-2 shows the experiment arrangement for binder tests

Table 2-2 Experiment design for different binder and their combination investigation

Test No.	Binder	Formula	Flow rate
1	15wt% Ludox	6 g Adsorbent + 2.5 g Ludox	180 mL/min
2	10wt% NB	10 g Adsorbent + 3.44 g NB	180 mL/min
3	7wt% Ludox and 5wt% Actigel	10 g Adsorbent +1.75 g Ludox +0.5 g Actigel	180 mL/min
4	12wt% NB and 3wt% Actigel	10 g Adsorbent +4.14 g NB + 0.3 g Actigel	180 mL/min

2.3 Results and discussion

Figure 2-3 shows ethylene and ethane adsorption isotherms at 25°C for Na-ETS-10 up to a pressure of 200 kPa. The curve for ethylene is more rectangular shaped than ethane, which implies a stronger interaction between ethylene and Na-ETS-10 exists, and the curves also reflect that the Na-ETS-10 has a higher capacity for ethylene than ethane.

Figure 2-4 shows ethylene and ethane adsorption isotherms at 25°C for Zn-RPZ up to a pressure of 200 kPa. In Figure 2-4, the curve for ethylene is also more rectangular shaped than ethane, but its capacity is less than Na-ETS-10. In the low pressure region, Na-ETS-10 has a limiting selectivity of 12 and Zn-RPZ has a limiting selectivity of 38.

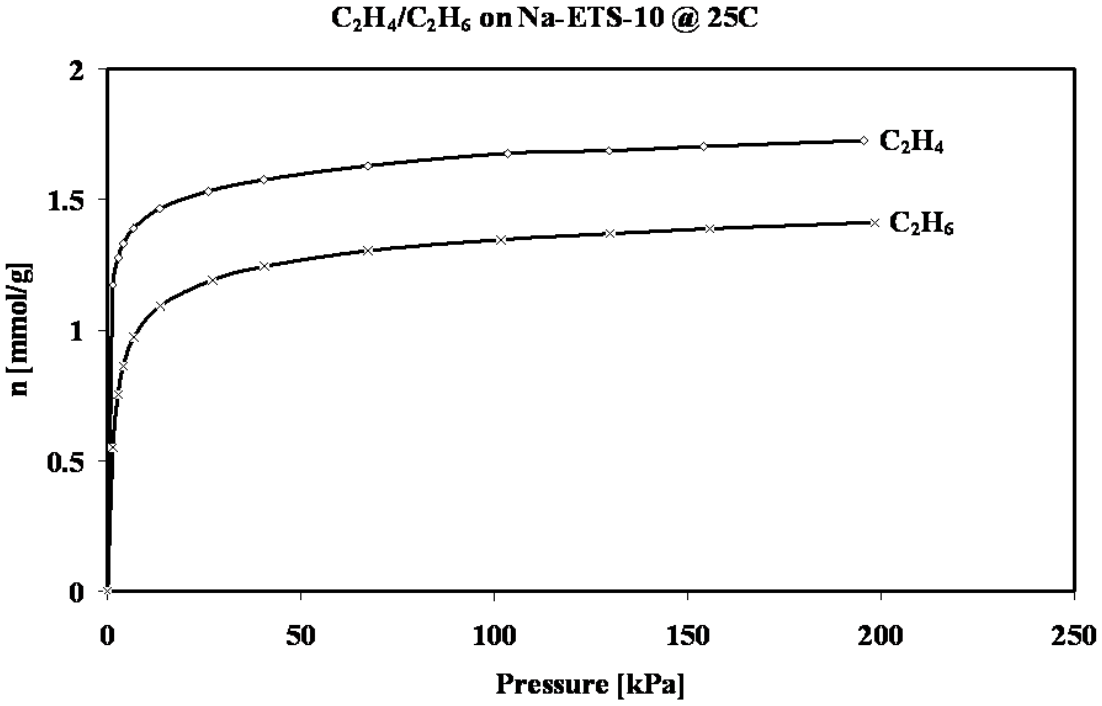

Figure 2-3 Ethylene and ethane adsorption isotherms at 25°C for Na-ETS-10

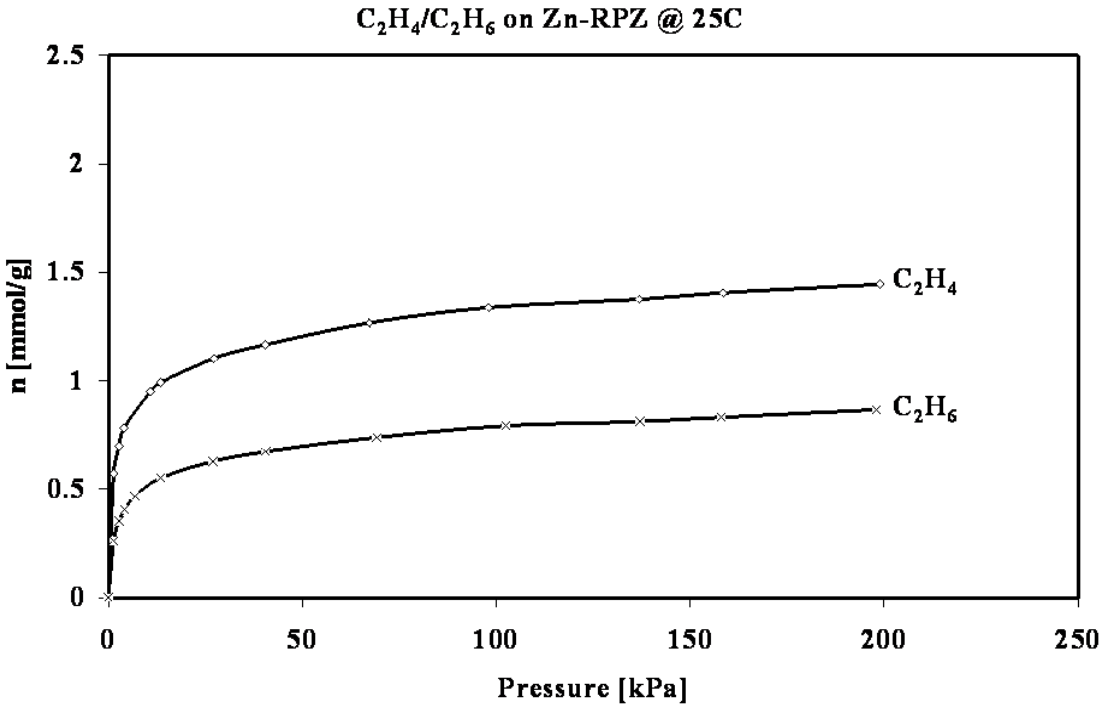

Figure 2-4 Ethylene and ethane adsorption isotherms at 25°C for Zn-RPZ

IGC analysis shown in Figure 2-5c illustrates the separation of 1mL of a 59-41% C_2H_4-C_2H_6 mixture on the Na-ETS-10 at 70°C. Compared to the pure gas chromatographic data (Figure 2-5a and 2-5b), it is clear that the first peak represents C_2H_6, while the second peak represents C_2H_4. The result demonstrates that Na-ETS-10 has a selectivity of 7.2 for C_2H_4/C_2H_6 at 70°C, which also implies that at low temperatures, such as ambient condition, the adsorbent has higher selectivity for C_2H_4/C_2H_6. C_2H_4 and C_2H_6 IGC analysis were also measured at 100°C and 130°C which were used to estimate the limiting isosteric heats of adsorption by means of the van't Hoff equation. IGC results for

these two temperature points are shown in Figure 2-6 and Figure 2-7. The retention times, Henry's Law constants and limiting selectivity are shown in Table 2-3, all of these values increase as the temperature decreases, as predicted by previous modelling of single-component isotherms (Anson et al., 2008; Kuznicki et. al, 2009). The heat of adsorption for C_2H_4 (50 KJ/mol) is higher than that for C_2H_6 (30 KJ/mol), which demonstrates that Na-ETS-10 is favorable for ethylene over ethane. Based on the data at these three temperatures, we can extrapolate the limiting selectivity to 30°C, indicating a limiting selectivity of 12.6 at 30°C. This information exactly illustrates the thermodynamic equilibrium effect of C_2H_4/C_2H_6 on Na-ETS-10. Because the pore size of ETS-10 has an average kinetic diameter of ~8 Å, which is larger than the molecular diameters of both C_2H_4 and C_2H_6 (4.163 Å and 4.443 Å, respectively), both of these two components can enter the inside of Na-ETS-10, while C_2H_4 has a double bond which allows C_2H_4 has a strong interaction with Na-ETS-10, much stronger than the interaction between C_2H_6 and Na-ETS-10.

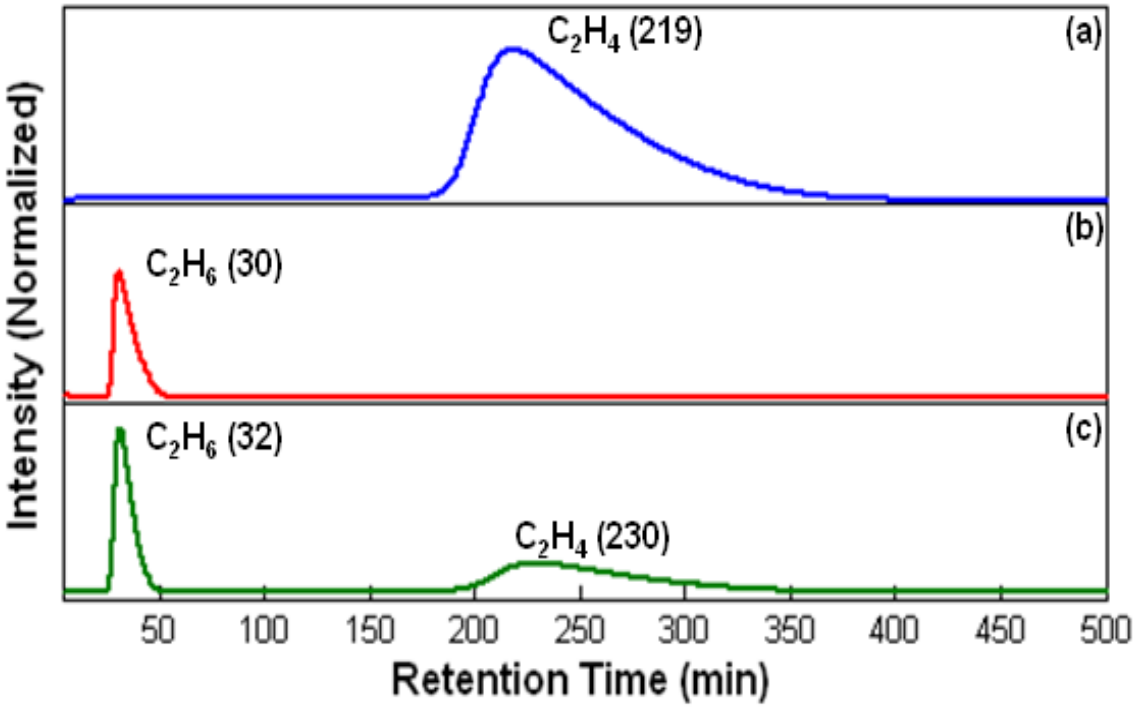

Figure 2-5 IGC analysis for ethylene and ethane on Na-ETS-10 at 70°C, (a) pure ethylene, (b) pure ethane, (c) mixture of 59% ethylene and 41% ethane

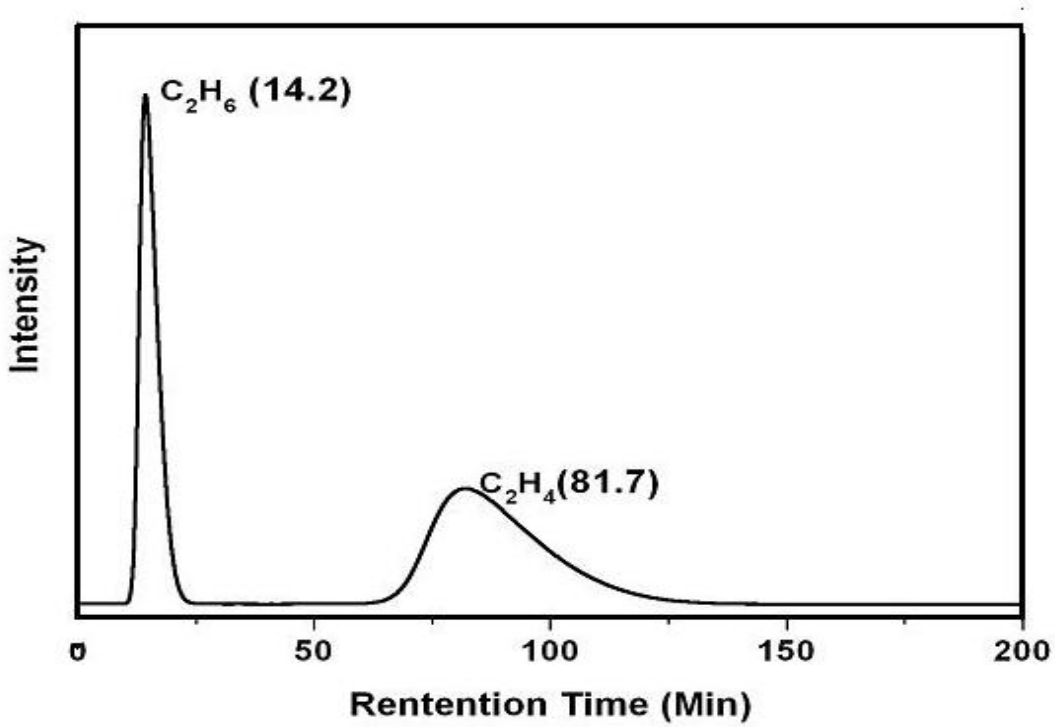

Figure 2-6 IGC analysis for mixture of 59% ethylene and 41% ethane on Na-ETS-10 at 100°C

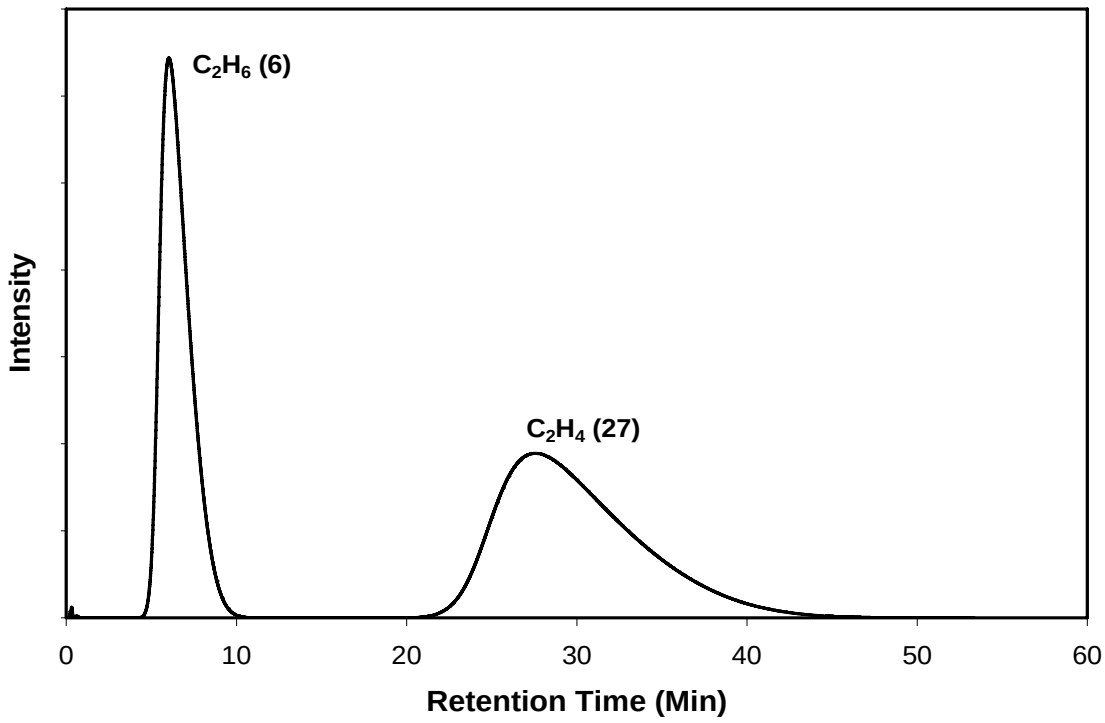

Figure 2-7 IGC analysis for mixture of 59% ethylene and 41% ethane on Na-ETS-10 at 130°C

Table 2-3 IGC retention times, Henry's Law constant (K) and limiting selectivity (α) for C_2H_4/C_2H_6 separation on Na-ETS-10

Temperature	Retention Time (min)*		K		α
	C_2H_4	C_2H_6	C_2H_4	C_2H_6	C_2H_4/C_2H_6
130°C	27.84	6.03	260.85	55.04	4.73
100°C	81.74	14.25	769.34	132.64	5.80
70°C	304.19	39.27	2867.92	368.68	7.78
30°C (extrapolated)	-	-	25202.46	2001.16	12.59

*Retention times represent the average of three separate experiments.

The results of IGC analysis in Figure 2-8 illustrate the separation of 1 mL of a 59-41% C_2H_4- C_2H_6 mixture on Zn-RPZ at 70°C. The first peak represents C_2H_6, while the second peak represents C_2H_4. The result demonstrates that Zn-RPZ also has the selective separation of C_2H_4/C_2H_6 at 70°C, which also can illustrate that in ambient condition, the adsorbent has higher selectivity for C_2H_4/C_2H_6. C_2H_4 and C_2H_6 IGC analysis were also respectively measured at 100°C and 130°C which were used to estimate the limiting isosteric heats of adsorption by means of the the van't Hoff equation. The IGC results for these two temperatures are shown in Figure 2-9 and Figure 2-10. The retention times, Henry's Law constants and limiting selectivity are also shown in Table 2-4. Based on this information, we can calculate the heat of adsorption for C_2H_4 and C_2H_6 respectively: 44.16 KJ/mol for C_2H_4 and 25.56 KJ/mol for C_2H_6. The heat of adsorption for C_2H_4 (44.16 KJ/mol) is higher than that for C_2H_6 (25.56KJ/mol), which demonstrates that Zn-RPZ favorably adsorbs ethylene over ethane.

These results exactly illustrate steric effect separation of C_2H_4/C_2H_6 on Zn-RPZ. Because the pore size of Zn-RPZ is larger than the C_2H_4 molecule and smaller than the C_2H_6 molecule, C_2H_6 was excluded from the internal adsorption sites of the adsorbent, and was not strongly adsorbed, while C_2H_4 can reach the internal adsorption sites and interact with the adsorbent.

Comparing IGC results of Zn-RPZ and Na-ETS-10, at a specific temperature condition (70°C, 100°C or 130°C), although the limiting selectivity on Zn-RPZ is higher than on Na-ETS-10, the two peaks of ethane and ethylene on Zn-RPZ can not split completely, while the two peaks of ethane and ethylene on Na-ETS-10 split very well. This implies Na-ETS-10 can more efficiently separate ethylene and ethane.

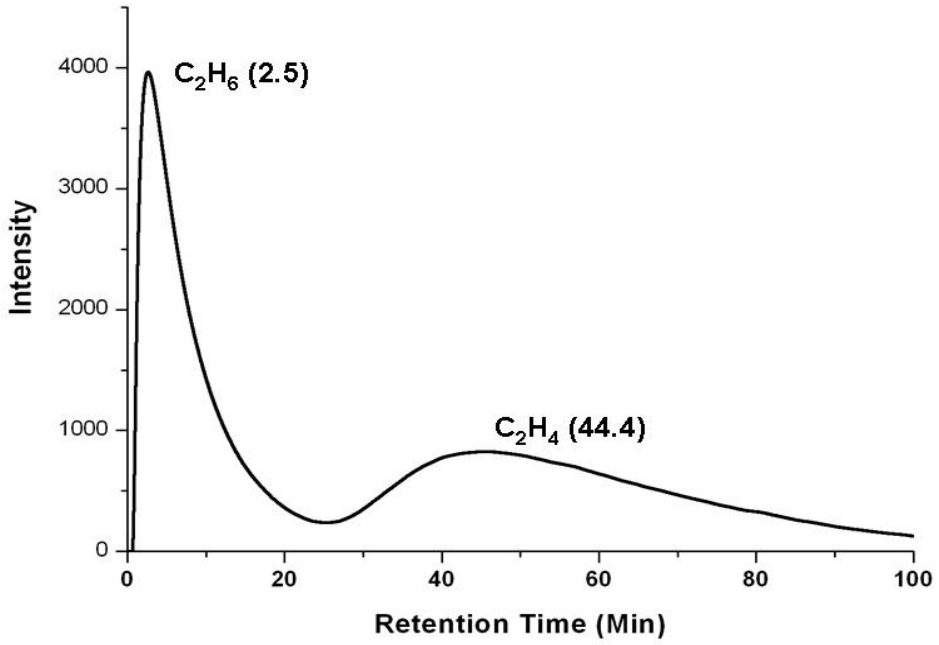

Figure 2-8 IGC analysis for mixture of 59% ethylene and 41% ethane on Zn-RPZ at 70°C

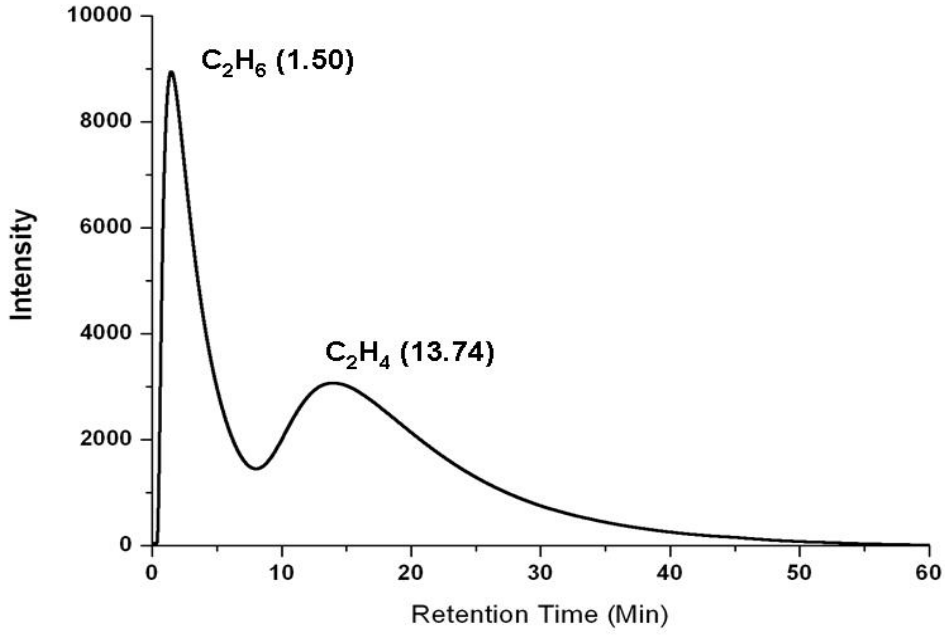

Figure 2-9 IGC analysis for mixture of 59% ethylene and 41% ethane on Zn-RPZ at 100°C

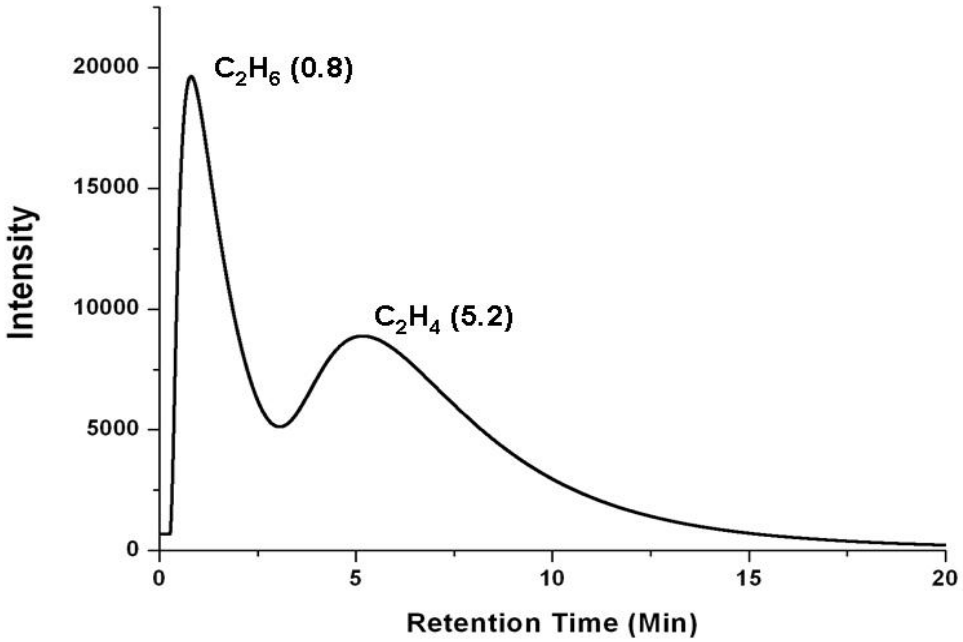

Figure 2-10 IGC analysis for mixture of 59% ethylene and 41% ethane on Zn-RPZ at 130°C

Table 2-4 IGC retention times, Henry's Law constant (K) and limiting selectivity (α) for C_2H_4/C_2H_6 separation on Zn-RPZ

Temperature	Retention Time (Min)*		K		α
	C_2H_4	C_2H_6	C_2H_4	C_2H_6	C_2H_4/C_2H_6
130°C	5.2	0.8	58.38	7.15	8.16
100°C	13.74	1.5	159.69	14.77	10.81
70°C	44.4	2.5	510.23	27.92	18.27
30°C (extrapolated)	-	-	3481.16	80.51	43.23

*Retention times represent the average of three separate experiments.

From the C_2H_4/C_2H_6 breakthrough curve for Na-ETS-10 shown in Figure 2-11, a pulse of pure C_2H_6 was obtained after 4 min of continuous gas flow. During this time, the adsorbents should yield a high concentration of C_2H_6. This information can help us design cycle times to optimize the amount of pure C_2H_6 recovery. After 16 min of continuous flow, the concentration of the outlet gas begins to reflect the inlet composition, therefore indicating that the Na-ETS-10 adsorbents have reached saturation and dynamic equilibrium. At this instance, the gas adsorbed by the materials has the highest concentration of C_2H_4. By injecting some water into the chamber, the adsorbed phase gas was quickly desorbed by the liquid water. The reason is because the interaction between water and the titanosilicate is much stronger than the interaction between ethylene (or ethane) and titanosilicate, so water can easily replace ethylene (or ethane). After injecting 10 mL water, there was no gas coming out anymore, and we can collect totally 1200 mL gas in the flask. And taking the sample to analyze in the GC, the composition of the desorbed gas is 87% C_2H_4 and 13% C_2H_6, which is reflected in Figure 2-13. As a comparison, the composition of the feed gas is also illustrated in Figure 2-12.

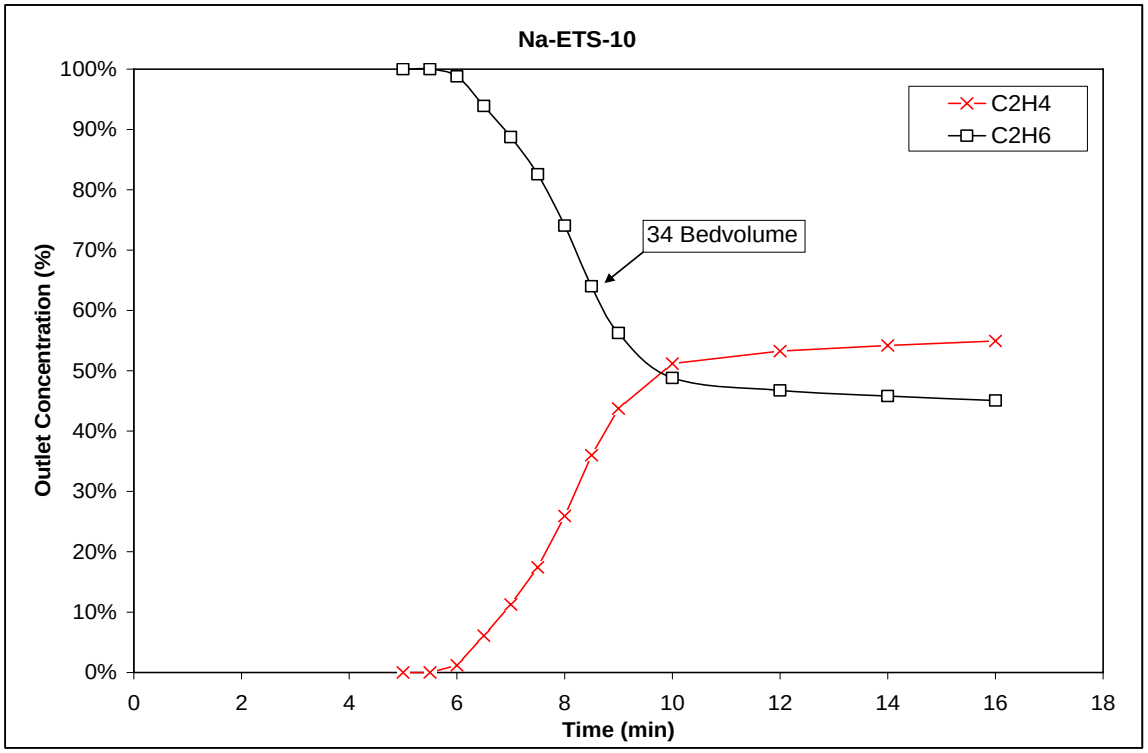

Figure 2-11 C_2H_4/C_2H_6 breakthrough curve on Na-ETS-10 with binder of 15wt% Ludox under a flow rate of 180 mL/min.

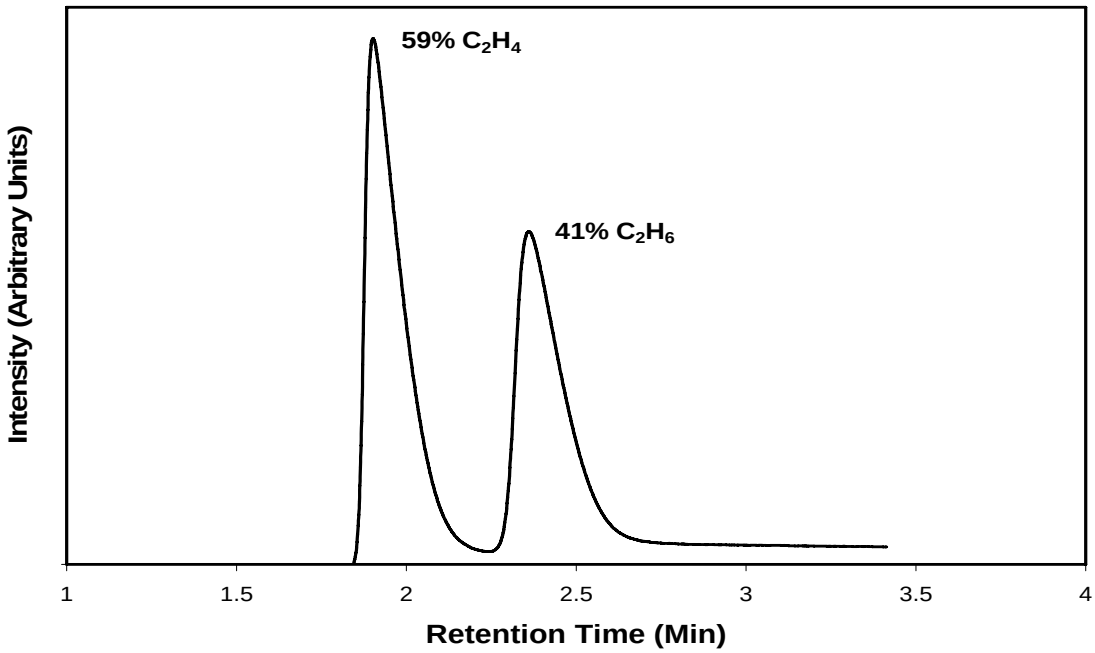

Figure 2-12 IGC analysis of composition of input gas

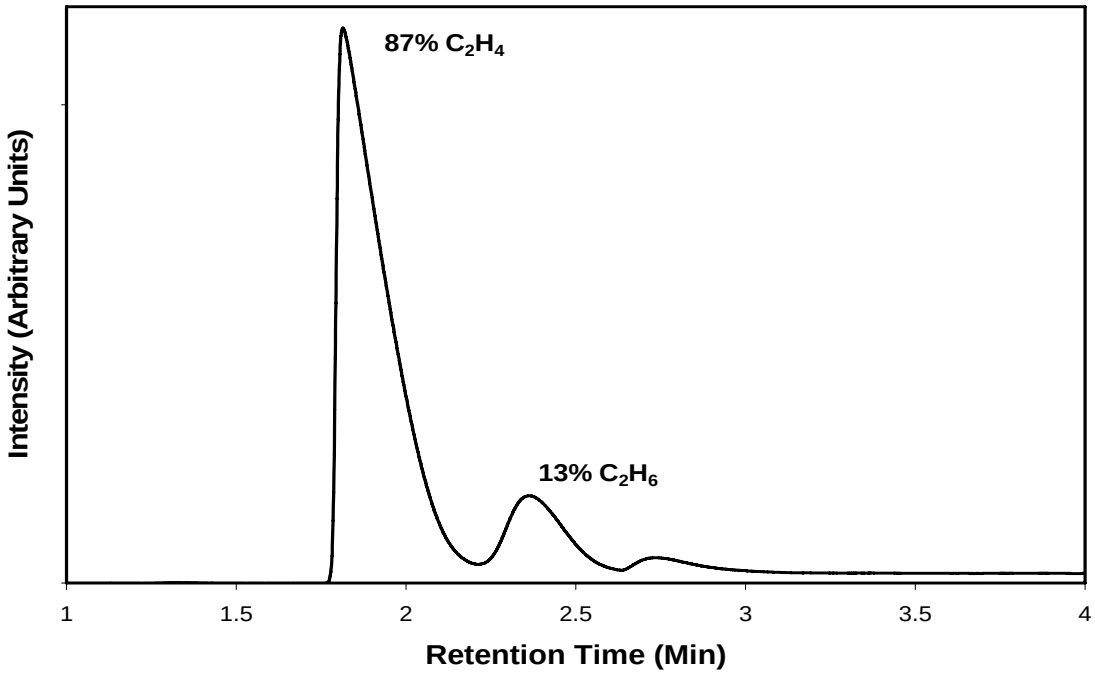

Figure 2-13 IGC analysis of composition of adsorbed phase gas on Na-ETS-10 at ambient condition and flow rate of 180 mL/min

From the C_2H_4/C_2H_6 breakthrough curve for Zn-RPZ shown in Figure 2-14, highly enriched C_2H_6 (approximate 90%) was observed after 1 min of flow. After 10 min of continuous flow, the concentration of the outlet gas begins to reflect the inlet composition, therefore indicating that the Zn-RPZ adsorbents have reached saturation and dynamic equilibrium. At this instance, the gas adsorbed by the materials has highest concentration of C_2H_4. By injecting some water into the chamber, the adsorbed phase gas was quickly desorbed by the liquid water. This water desorption procedure was described in the Na-ETS-10 section. After injecting about 10 mL water, there was no gas coming out anymore, and we can collect totally 610 mL gas in the flask. A sample was taken for analysis in the GC. The composition of the desorbed gas is 81.8% C_2H_4 and 18.2% C_2H_6, which is reflected in Figure 2-15.

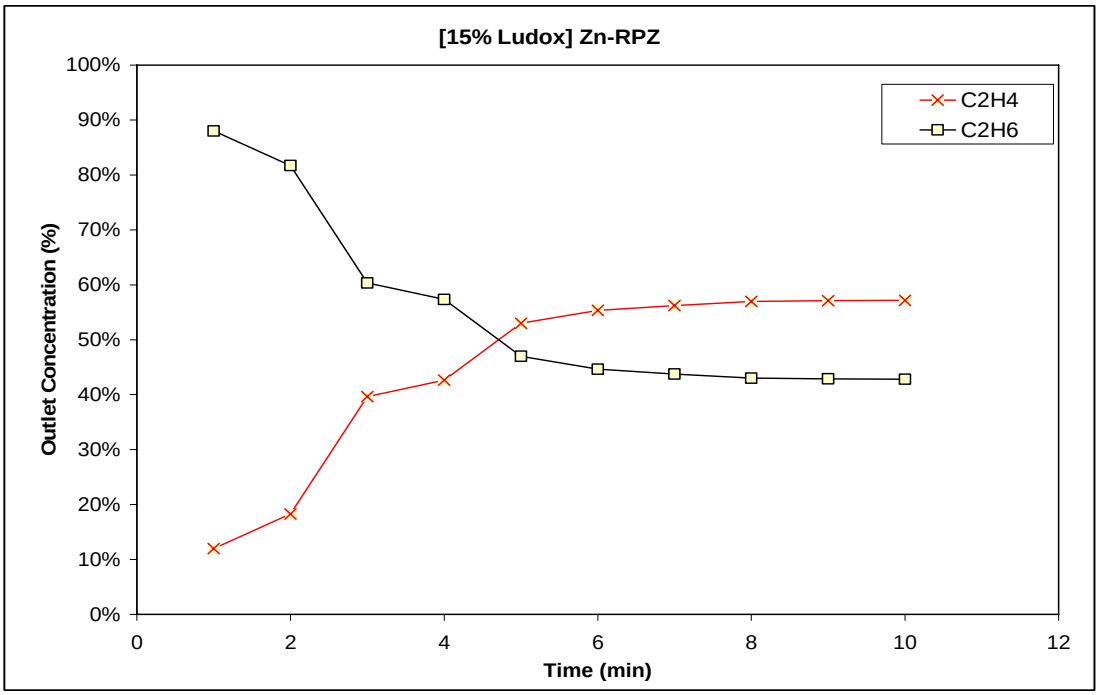

Figure 2-14 C_2H_4/C_2H_6 breakthrough curve on Zn-RPZ with binder of 15wt% Ludox under the flow rate of 180 mL/min.

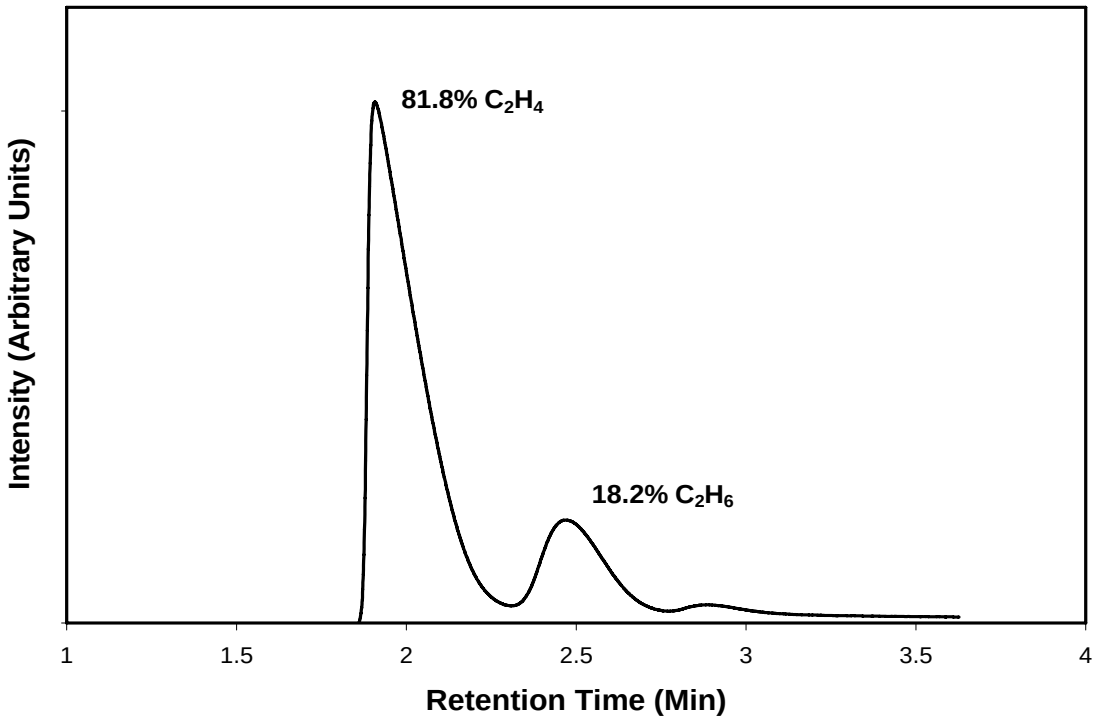

Figure 2-15 IGC analysis of composition of adsorbed phase gas on Zn-RPZ

Table 2-5 Adsorption performance comparison of Na-ETS-10 with Zn-RPZ

Performances	**Na-ETS-10**	**Zn-RPZ**
Limiting Selectivity based on Isotherms @ 25C	12	38
Limiting Selectivity based on IGC @ 30C	12.59	43.23
Composition of Adsorbed Phase Gas @25C	87% C2H4 13% C2H6	81.8% C2H4, 18.2% C2H6
Capacity @ 25C	1200 mL per 30 g	610 mL per 30 g
Binary bed selectivity @ 25C	4.65	3.12

From Table 2-5, we can conclude that, although the limiting selectivity of Zn-RPZ calculated from the data from the isotherm and the IGC is higher than Na-ETS-10, in a practical lab-scale test the binary bed selectivity of Na-ETS-10 is higher, producing higher purity ethylene and having much higher capacity.

Table 2-6 Comparison of different binders

Raw Materials	**Binders**	**Density of Pellets**
Na-ETS-10	15wt% Ludox	0.734 g/mL
Na-ETS-10	10wt% NB	0.7 g/mL
Na-ETS-10	7wt% Ludox and 5wt% Actigel	0.667 g/mL
Na-ETS-10	12wt% NB and 3wt% Actigel	0.622 g/mL

Table 2-6 shows the difference between the different binder system, composition and density were compared. Actapulgite (actigel) is a pore former clay mineral that contracts upon thermal treatment. Upon activation at 350°C, the actapulgite clay contracts and introduces porosity in the composite ETS-10 material.

In the breakthrough curve in Figure 2-16, using pure sodium silicate as a binder, gas which contains approximate 70% C_2H_6 was observed after 6 min. We can not design a cycle system to collect high purity ethane from ETS-10 and this binder. Actigel was also added combined with ludox or sodium silicate. In Figure 2-17, 7wt% Ludox and 5wt% Actigel as binder can also get 100% ethane after 5 min, but the purity of ethane drops quickly compared with using pure Ludox as binder which shown in Figure 2-11. Figure 2-18 shows that 3wt% Actigel and 12wt% sodium silicate as binder can not produce pure ethane. Although it has a clear breakthrough trend, it is still not good for high purity ethane production.

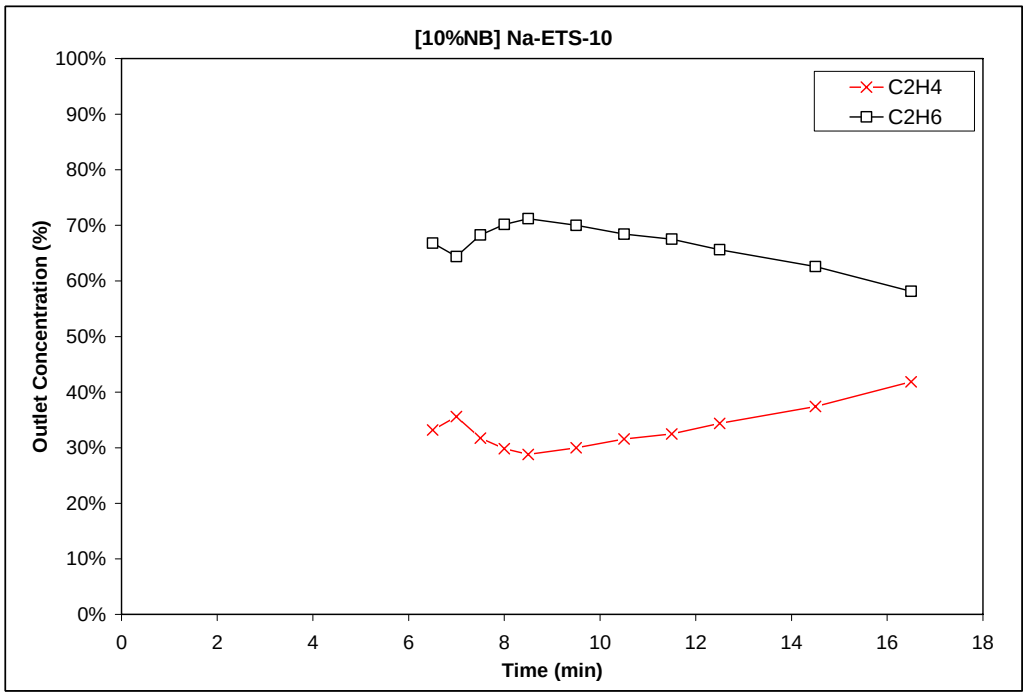

Figure 2-16 C_2H_4/C_2H_6 breakthrough curve on Na-ETS-10 with binder of 10wt% sodium silicate under the flow rate of 180 mL/min.

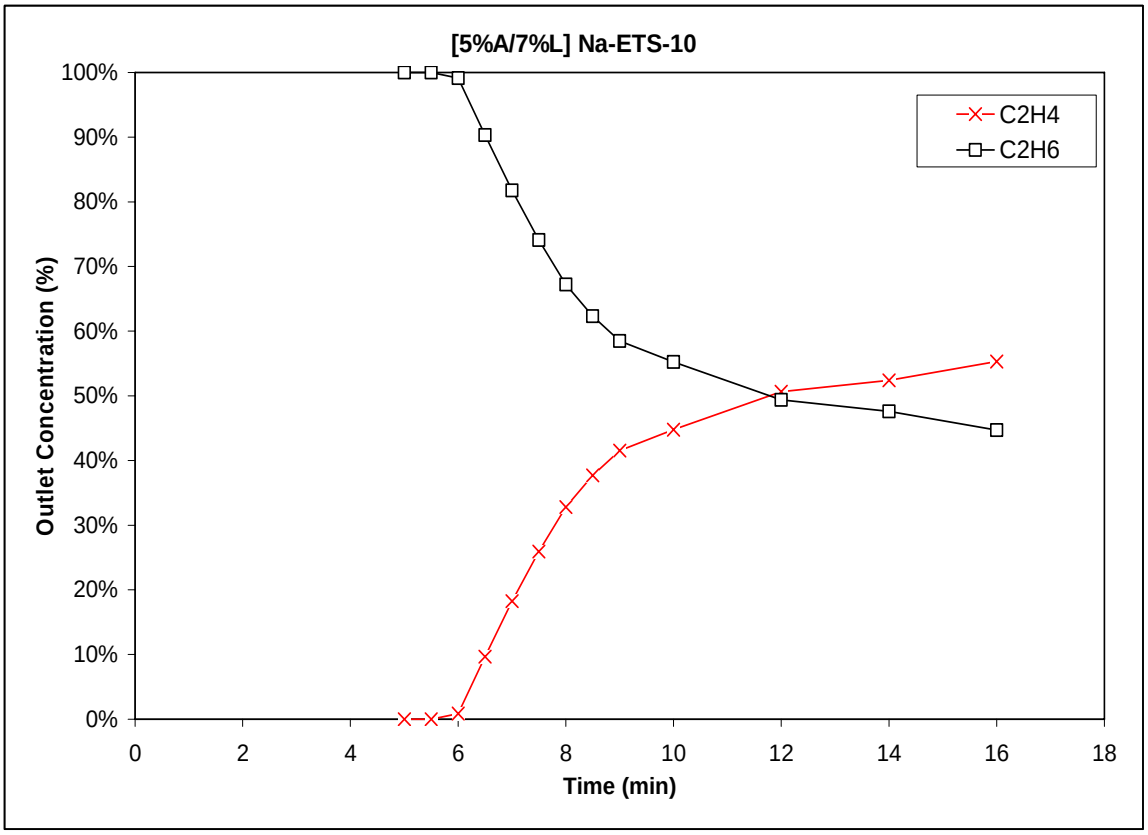

Figure 2-17 C_2H_4/C_2H_6 breakthrough curve on Na-ETS-10 with binder of 5wt% Actigel and 7wt% Ludox under the flow rate of 180 mL/min.

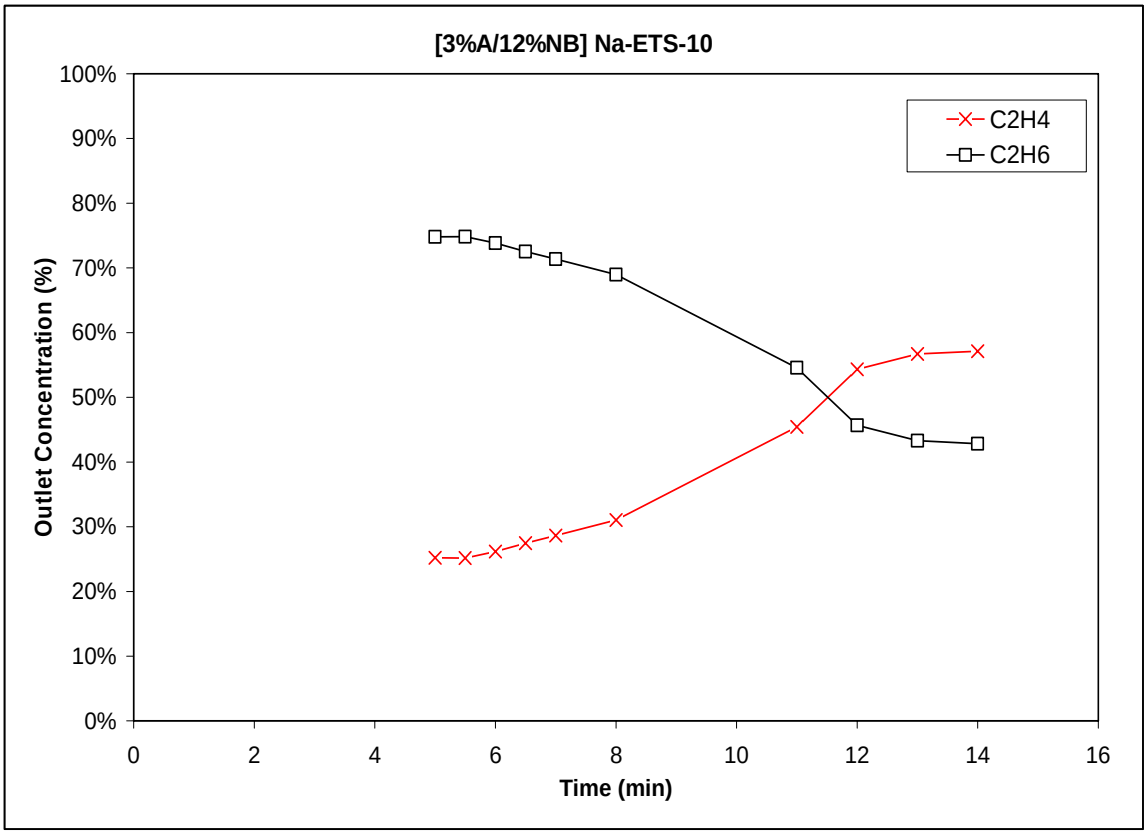

Figure 2-18 C_2H_4/C_2H_6 breakthrough curve on Na-ETS-10 with binder of 3wt% Actigel and 12wt% sodium silicate under the flow rate of 180 mL/min

The ethane/ethylene breakthrough profiles were also taken under different flow rates. Besides the flow rate of 180 mL/min tested before, 115, 250 and 400 mL/min were also investigated. Figures 2-19 to 2-21 illustrate that, under these flow rates, high purity ethane can not be obtained. This demonstrates that flow rate is very important in adsorptive separation. The flow rate of 180 mL/min should be used for best results using Na-ETS-10 as adsorbent and 15wt% Ludox as binder in our apparatus.

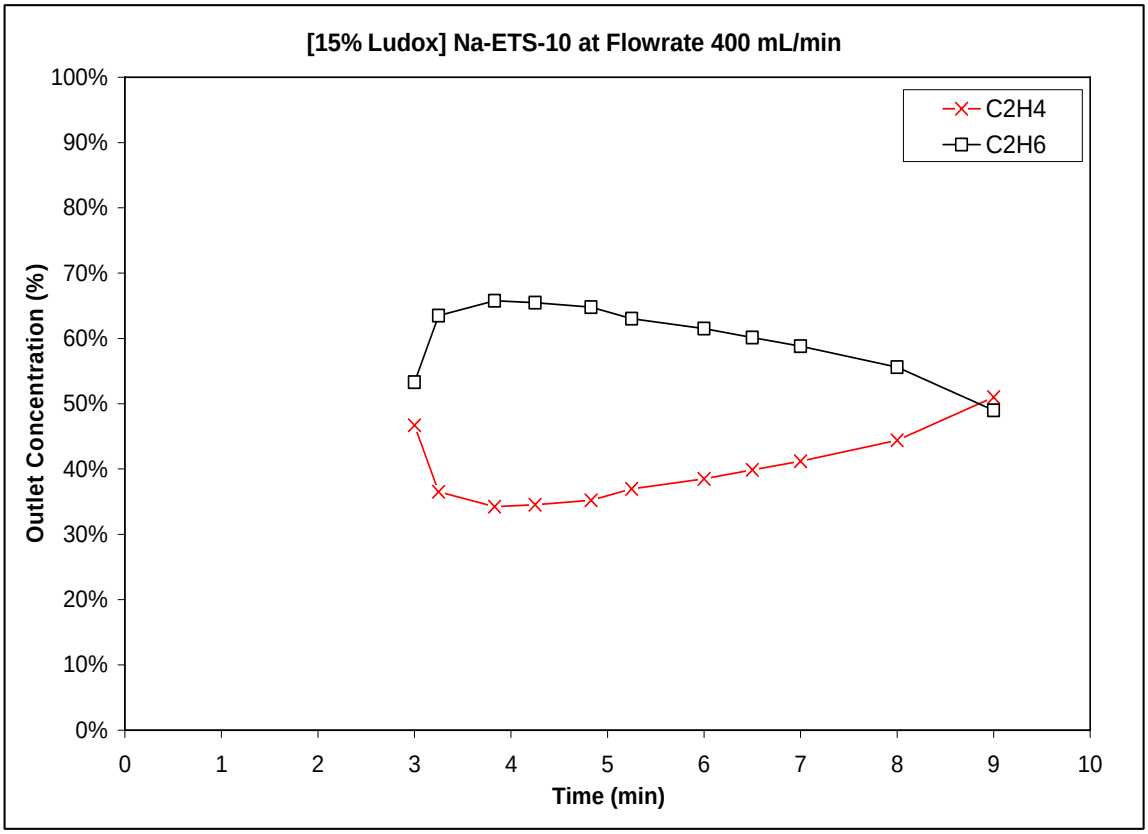

Figure 2-19 C_2H_4/C_2H_6 breakthrough curve on Na-ETS-10 with binder of 15% Ludox under the flow rate of 400 mL/min

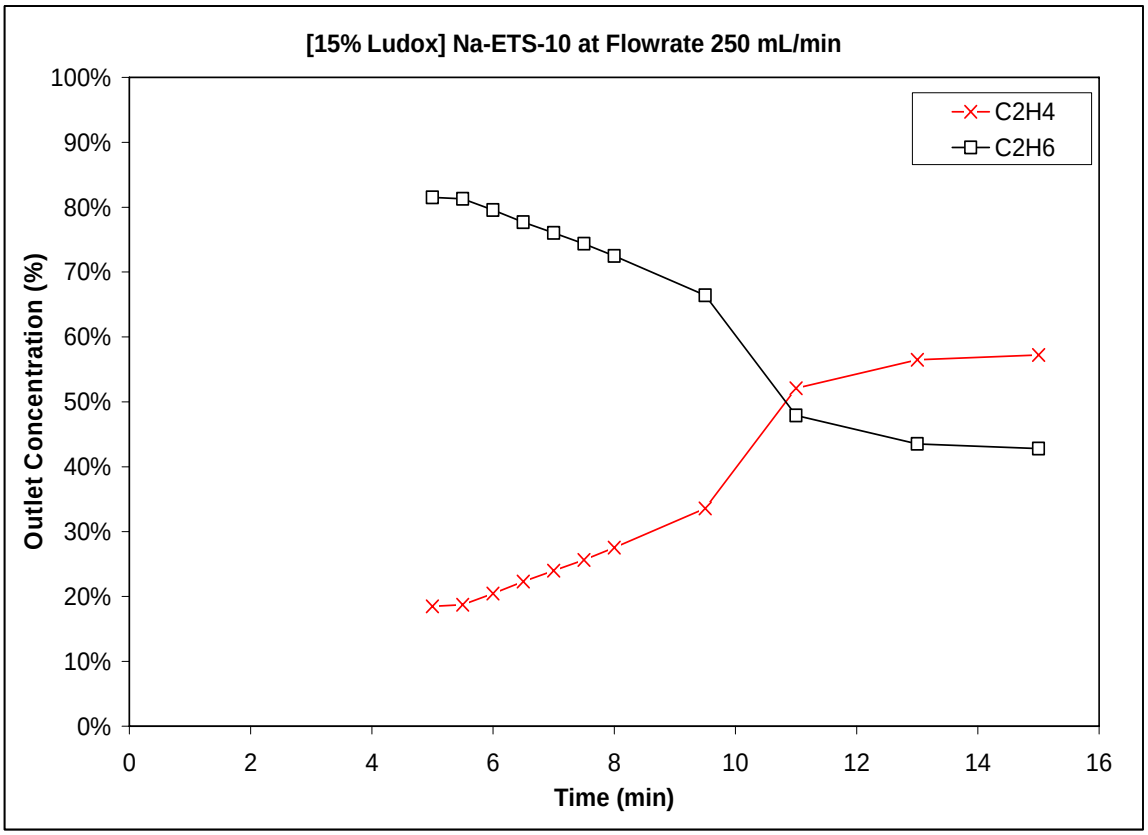

Figure 2-20 C_2H_4/C_2H_6 breakthrough curve on Na-ETS-10 with binder of 15wt% Ludox under the flow rate of 250 mL/min

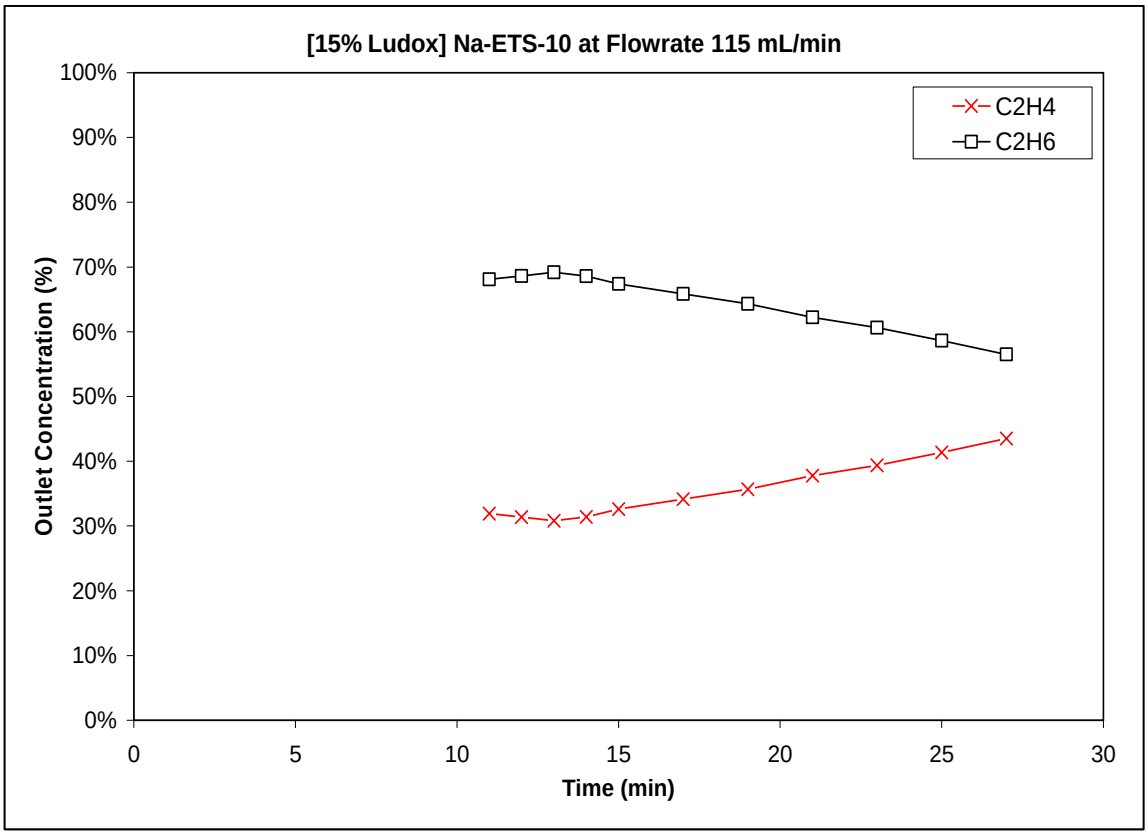

Figure 2-21 C_2H_4/C_2H_6 breakthrough curve on Na-ETS-10 with binder of 15wt% Ludox under the flow rate of 115 mL/min

2.4 Conclusion

From chromatographic, volumetric and gravimetric isotherm measurement, Na-ETS-10 demonstrates adsorptive selectivity for ethylene over ethane. We can conclude that, based on 30 g Na-ETS-10, due to the thermodynamic equilibrium effect, after the fully saturating the ETS-10 and desorption, we can produce a 1.2 L mixture containing 87% C_2H_4 and 13% C_2H_6, which gives a binary bed selectivity of 4.65. Based on 30 g Zn-RPZ, due to the molecular exclusion effect, we can produce a 610 mL mixture containing 81.8% C_2H_4 and 18.2% C_2H_6, which means we can get a binary bed selectivity of 3.12. It is clear that Na-ETS-10 has a higher capacity of adsorbed gas, and gives a higher purity of ethylene. Na-ETS-10 is our first choice for ethylene and ethane separation. Using 15wt% of ludox as binder system and 180 mL/min as the flow rate of the feed gas, we can produce the best breakthrough curve profile, in which we can get the highest purity of ethane (100%) at the beginning of the breakthrough which is useful for the recycle use for the cracking feeds. Based on these conditions, we can design cycle times to optimize the amount of pure C_2H_6 recovery.

Chapter 3 C_2H_4/C_2H_6 separation under high pressure and low temperature

3.1 Introduction

Considering ethylene plant working conditions, it is preferred to run ethylene and ethane separations under low temperature and high pressure. Based on the adsorption theory, we know that by decreasing the temperature of the adsorption, the selectivity of the adsorbent for ethylene over ethane will increase. This means running at low temperature will benefit ethylene enrichment. From the isotherm, we also know that the capacity of the adsorbent will also increase. Based on these two reasons, we can predict that high pressure and low temperature can improve the ethylene and ethane separation. In this chapter, a practical high pressure low temperature binary bed system will be investigated.

3.2 Experimental

High pressure isotherms were run at 0°C and 20°C for ethane and ethylene using a HPVA-100 system constructed by VTI Corp. of Hialeah, FL. Test samples were dried at 200^{o}C for 6 h under a vacuum of greater than 10^{-4} Torr. Buoyancy effects were corrected with a helium displacement isotherm taken at the same temperature as the respective ethylene and ethane isotherms. In this experiment, the low temperature is 0°C, which is easily prepared by a ice-water mixture. The maximum pressure of the isotherm is 2000 kPa.

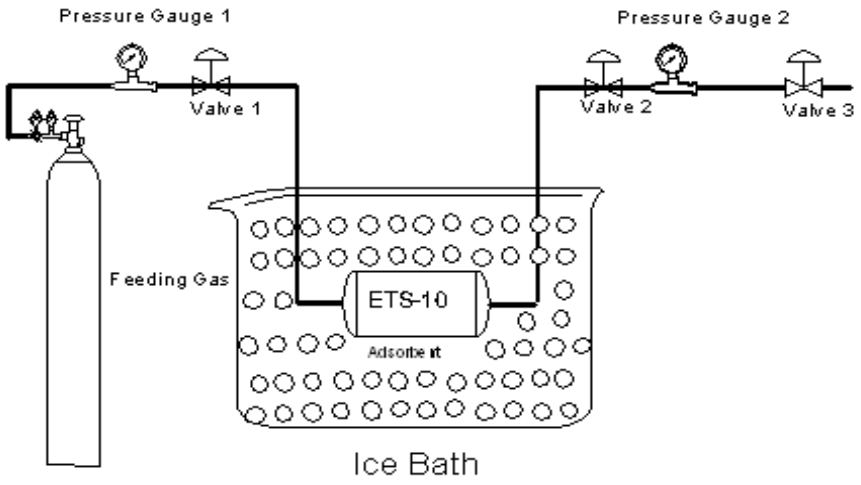

Figure 3-1 Experimental schematic of high pressure and low temperature adsorption process

To figure out how the pressure and temperature affects the adsorption and separation, four sets of experiment conditions were tested, 1 atm-25°C, 4 atm-25°C, 1 atm-0°C and 4 atm-0°C. After these experiments, higher pressure test was taken at 8 atm-0°C. In total 3 different pressures (1 atm, 4 atm, and 8 atm) were tested.

As Figure 3-1 illustrates, the high pressure is generated by the feed gas cylinder. The two pressure gauges on both side of the chamber are used to make sure the adsorbent is under a specific pressure which is supplied by the feed gas cylinder. Valve 3 after pressure gauge 2 is used to control the flow rate of the gas in the unit, which requires fine control. We can get a quick prediction of how fast the gas comes out by observing the bubbles in the water at the exit. The chamber which contains the adsorbent was kept in an ice water

bath.

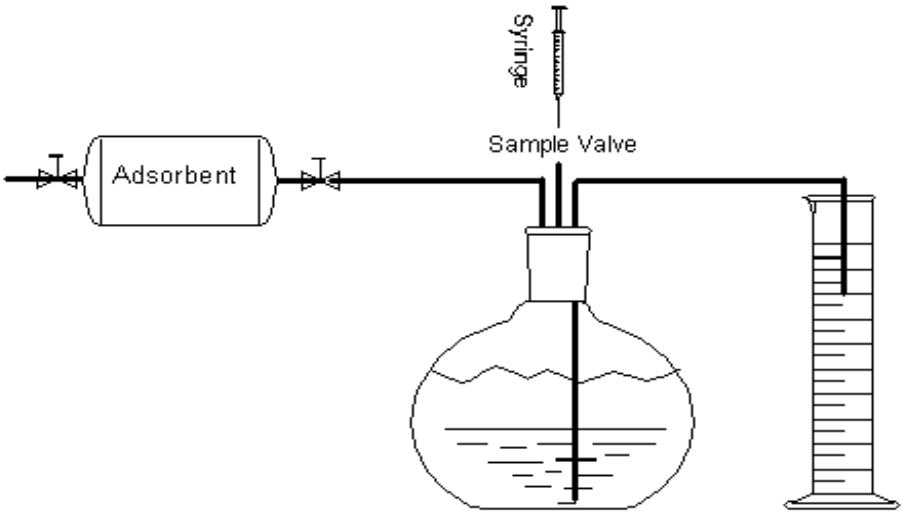

Figure 3-2 Experimental schematic of gas collection under pressure release

After the system has reached equilibrium, the two valves at both sides of the chamber are closed at the same time (which ensures the chamber maintains high pressure inside), and then the chamber is removed from the assembly in Figure 3-1.

Because of the high pressure, the desorption procedure contains two steps:

Step one is illustrated in Figure 3-2. The chamber is connected with the gas collection assembly. After turning on the valve, some gas will be released into the flask. This first part of the gas comes from the free space between the adsorbent pellets. After the pressure inside of the chamber reaches ambient pressure, we use a syringe to collect a sample and analyze it in the GC. The graduate cylinder is used to measure the volume of this part of gas, which is denoted V_1.

Step two is the same as discussed in chapter 2, which uses water to desorb the adsorbed

phase gas. The volume of the gas desorbed by water was measured and the composition was analyzed by GC. This volume is denoted V_2.

3.3 Results and discussion

Figure 3-3 shows ethylene and ethane adsorption isotherms at 0°C (and 20°C) for Na-ETS-10 up to a pressure of 2000 kPa. With the temperature decreasing from 20°C to 0°C, the capacity of both ethylene and ethane increases. At a specific temperature, the capacity increases with pressure.

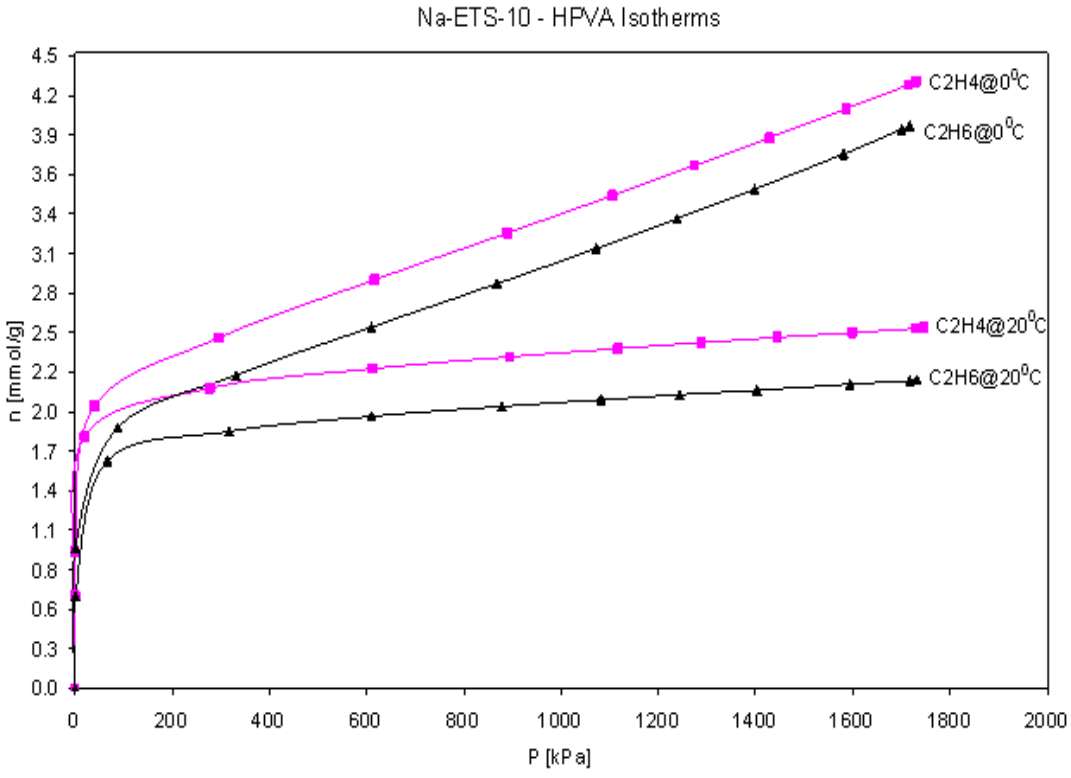

Figure 3-3 High pressure isotherm for C_2H_4 and C_2H_6 on Na-ETS-10 under 0°C and 20°C

Table 3-1 Composition of gas desorbed for 1 atm-25°C, 4 atm-25°C, 1 atm-0°C and 4 atm-0°C

	Conditions	Na-ETS-10 With Ludox (15%SiO_2) 45cc,30g	Selectivity
Group 1	4 atm 0°C	V_1=336 mL (60.4% C_2H_4) **V_2=1460 mL (89.2% C_2H_4)**	**5.74**
Group 2	1 atm 0°C	**V_2=1430 mL (87.09% C_2H_4)**	**4.68**
Group 3	4 atm 25 °C	V_1=268 mL (62.26% C_2H_4) **V_2=1390 mL (89% C_2H_4)**	**5.62**
Group 4	1 atm 25°C	**V_2=1280 mL (87% C_2H_4)**	**4.65**

In Table 3-1, V_1 is the volume of gas collected after pressure release, V_2 is the volume of gas collected by water desorption. Comparing group 3 and group 4, we discover that increased pressure causes capacity increase from 1280 mL to 1390 mL, and the selectivity also increase. The selectivity increase is shown by the ethylene composition increasing from 87% to 89%.

Comparing group 1 and group 3, we found that under the same pressure, decreasing the temperature, caused the capacity increase from 1390 mL to 1460 mL, and the ethylene composition increases from 89% to 89.2% which shows that the selectivity of ethylene over ethane is increasing.

Table 3-2 Composition of gas desorbed for 1 atm-0°C, 4 atm-0°C and 8 atm-0°C

	Conditions	Na-ETS-10 With Ludox (15%SiO_2) 45cc,30g	Selectivity
Group 1	8atm 0 °C	V_1=635 mL (60.22% C_2H_4) **V_2=1584 mL (92.96%C_2H_4)**	**9.17**
Group 2	4atm 0°C	V_1=336 mL (60.4%C_2H_4) **V_2=1460 mL (89.2%C_2H_4)**	**5.74**
Group 3	1 atm 0°C	**V_2=1430 mL (87.09% C_2H_4)**	**4.68**

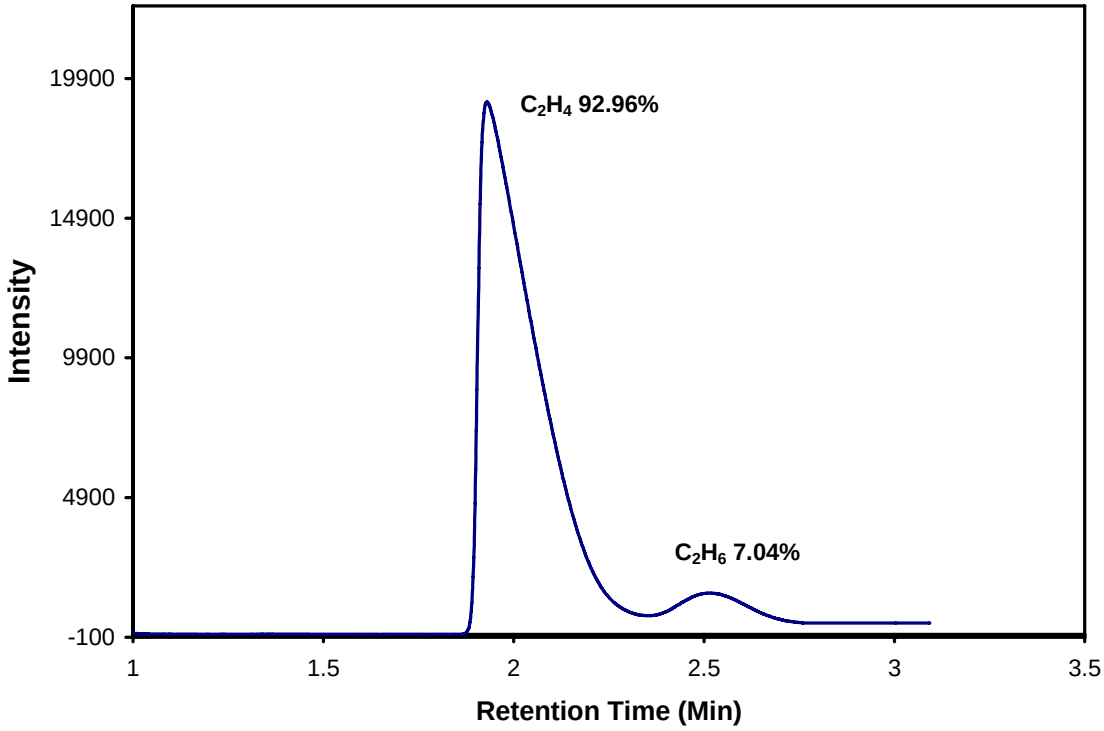

Figure 3-4 IGC analysis for composition of adsorbed phase (V_2) under 8 atm and 0^oC

From Table 3-2, we can see that at the same temperature, V_1 increases with the trend of the pressure, which matches the equation *PV=nRT*, because the free space between the adsorbent pellets and the chamber is constant. The capacity of the adsorption V_2 also

continuously increases with the pressure from 1430 mL to 1583 mL. Increasing the pressure causes more and more molecules of ethylene and ethane to enter the interior channels of the adsorbent in addition to the surface. Ethylene which has double bond of carbon was strongly adsorbed by the material, dominating the adsorbed gases. Even after releasing the pressure, most of the adsorbed phase gas still stays on the adsorbent, resulting in the V_1 composition remaining the same when pressure is increased. At higher pressure, ethylene is easier to be selective adsorbed by the adsorbent, which was reflected by the ethylene concentration is increasing in V_2. Due to these reasons, we can produce 1584 mL of gas having a composition of 92.96% C_2H_4 using approximately 30 g of adsorbent. This result was illustrated in Figure 3-4. It is an obvious improvement from the result under ambient conditions. Further tests were also run under 180 psi and 350 psi, while the concentration of ethylene stays between 90% and 91% which has a drop compared with 120 psi, indicates that the selectivity of ethylene will reach a stable number when pressure is increasing.

3.4 Conclusion

From the isotherms and the tables, we can conclude that both high pressure and low temperature favors C_2H_4/C_2H_6 selectivity and increases the C_2H_4 adsorption capacity. Using 30 g of Na-ETS-10, under ambient pressure and room temperature, 1280 mL of gas having a composition of 87% C_2H_4 was obtained with a binary bed selectivity of 4.65; at 8 atm and 0°C, 1584 mL of gas having a composition of 92.96% C_2H_4 was obtained with a binary bed selectivity of 9.17. High pressure and low temperature is a clear improvement over ambient pressure and temperature conditions.

Chapter 4 Desorption methods comparison

4.1 Introduction

From Figure 2-5 in chapter 2, the IGC results show that at 70°C, the retention time of ethylene is 230 minutes, which means the ethylene is strongly adsorbed by Na-ETS-10 at ambient condition, and at room temperature this time would be longer. An efficient and cost-effective desorption method is important in the C_2H_4 and C_2H_6 separation. From the isotherm of Figure 2-3 in Chapter 2, we see that the traditional PSA does not work for C_2H_4/C_2H_6 separation. The obvious solution should be thermal desorption, which can be one of our options. Usually water is not a practical method of desorption for traditional zeolite adsorbents, but based on the unique molecular structure of ETS-10, it is believed that ETS-10 can still adsorb ethylene and ethane even if it is not completely dry. Thomas A.J. Schweiger (1993) did research on steam regeneration of solvent adsorbents, using steam regeneration of activated carbon beds with adsorbed n-hexane. Steam is an effective regenerating agent for the adsorbent, because of its high heat content, it quickly raises the temperature of the adsorbent to desorb the solvent. Further, adsorbed water competes with adsorbed gas for pore volume of the adsorbent to enhance desorption. It would be ideal to use steam to desorb the gas and our adsorbent can be used to separate the C_2H_4 and C_2H_6 for the next cycle without any activation.

Another candidate for regeneration and desorption is the microwave method. Microwave energy is widely used in kitchen appliances to heat food by dielectric heating. This is accomplished by using microwave radiation to heat water and other polarized molecules within food.

Microwaves refer to the electromagnetic spectrum between 300 MHz and 300 GHz, with a corresponding wavelength between 1 m and 1 mm. Typically, domestic microwave ovens operate at 2,450 MHz (Meredith, 1998).

When frequencies of microwave are above 1 GHz, polarization is the dominant mechanism. Polarization is due to coupling of dipolar components of molecules with the alternating electric field which results in frictional losses depicted as heat.

Microwave heating results from the electric field being able to polarize the charges in the material that is subject to the microwave, and the inability of this polarization to follow the extremely rapid reversal of the electric field caused by the microwave. Molecules with symmetric charge distribution are non-polar, have a very small dipole moment, and exhibit limited absorption of microwaves. In contrast, water and a wide range of organic compounds are polar since they have charge asymmetry, they have large dipole moments and absorb microwave energy (Hashisho, 2007).

As an illustration of this phenomenon, a kitchen microwave oven works by passing non-ionizing microwave radiation through the food. Water, fat, and other substances in the food absorb energy from the microwave in a process called dielectric heating. Many molecules (such as water) are electric dipoles, meaning that they have a positive charge at one end and a negative charge at the other, and therefore rotate as they try to align themselves with the alternating electric field of the microwaves. This molecular movement creates heat which is then dispersed as the rotating molecules hit other molecules and put them into motion.

The main advantage of using microwave energy is that the whole process can be done in a relatively short period of time and also consume low amount of gas and energy. Robert

S. Inglis (1987) reported that porous desiccant material, such as silica gel, activated alumina, molecular sieves or mixtures thereof, can be efficiently regenerated for reuse as a drying agent by irradiating a bed of the desiccant materials with microwave energy. C.O.Ania (2004) also compared the microwave-induced regeneration of activated carbons with the conventional thermal regeneration. A detailed overview of these studies is presented in Table 4-1 by Hashisho (Hashisho, 2007).

Table 4-1 Microwave energy heating used in activating adsorbents (Hashisho, 2007)

Study	Scale	Adsorbent	Description
(Coss and Cha, 2000)	Bench	GAC	Performed bench-scale adsorption of MEK, acetone, and TCE on GAC. The adsorption reactor was moved into another reactor for microwave regeneration.
(Cha and Carlisle, 2001)	Pilot	GAC	Performed bench and pilot-scale adsorption of MEK on GAC. Regeneration was achieved by moving the GAC into another microwave reactor for microwave regeneration.
Price and Schmidt, 1997)	Bench	Molecular sieves (13X and 5A), Molsiv high silica zeolite (MHSZ) and Dowex Optipore	Performed bench-scale adsorption of MEK, toluene, and n-propyl acetate on molecular sieves (13X and 5A), Molsiv high silica zeolite (MHSZ) and Dowex Optipore V502. The adsorption column is moved into another reactor for microwave regeneration at low pressure.
(Kong and Cha, 1996; Kong and Cha, 1995)	Bench	Char, activated carbon and coke	Performed bench-scale adsorption of NO_x on six carbon adsorbents including char, activated carbon and coke. The NO_x-saturated adsorbent was regenerated by moving it into another reactor for microwave regeneration.
(Bradshaw *et. al.*, 1998)	Bench	GAC	Performed bench-scale microwave regeneration of spent GAC from the carbon-in-pulp (CIP) process used in the recovery of gold.
Reub *et. al.*, 2002	Bench	Zeolite and carbon-impregnated silica gel	Investigated dual-component adsorption and microwave regeneration of DAY (a hydrophobic zeolite) and Envisorb B+ (a silica gel with incorporated micro-dispersed activated carbon) using a fixed bed adsorption-regeneration system consisting of an adsorption column installed in a microwave reactor using 2,450 MHz microwaves.

4.2 Experimental

4.2.1 Thermal desorption

After the adsorbent reaches saturation, it is removed from the adsorption unit, and installed in the oven as shown in Figure 4-1. The temperature of the oven was set to 250°C and 300°C.

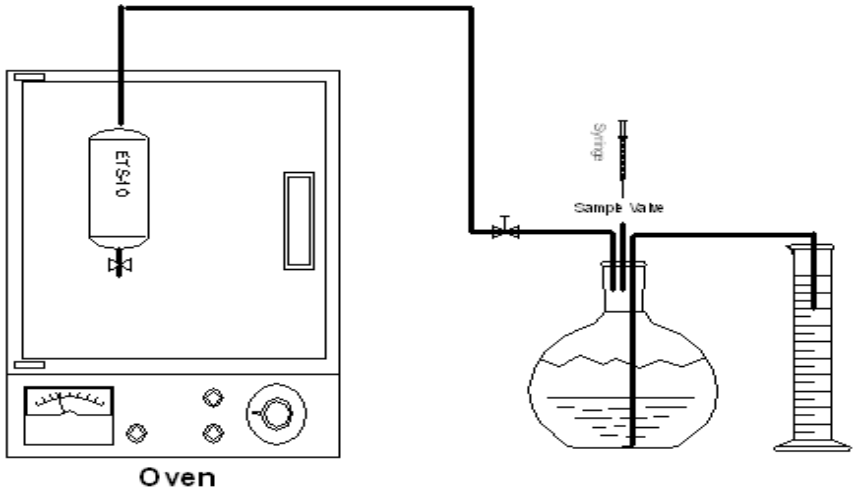

Figure 4-1 Experimental schematic of thermal desorption process

The volume of the gas released from the chamber was measured and tracked with time. The experiment was run under two different conditions (250°C and 300°C).

4.2.2 Steam desorption

Figure 4-2 illustrates the steam desorption process. Steam is initially generated in a flask on a heating mantle. The steam then passes through a column surrounded by rope heaters to raise the temperature of the steam to 200-400°C. A thermocouple is placed after the rope heaters to detect the temperature of the steam. To prevent water condensation within

the column, valves are placed at the inlet and outlet of the adsorbent column to control the amount of superheated steam passing through the column. The desorbed gas will displace a measurable amount of water from the round bottom flask into a graduated cylinder corresponding to the overall volumetric capacity of the adsorbent.

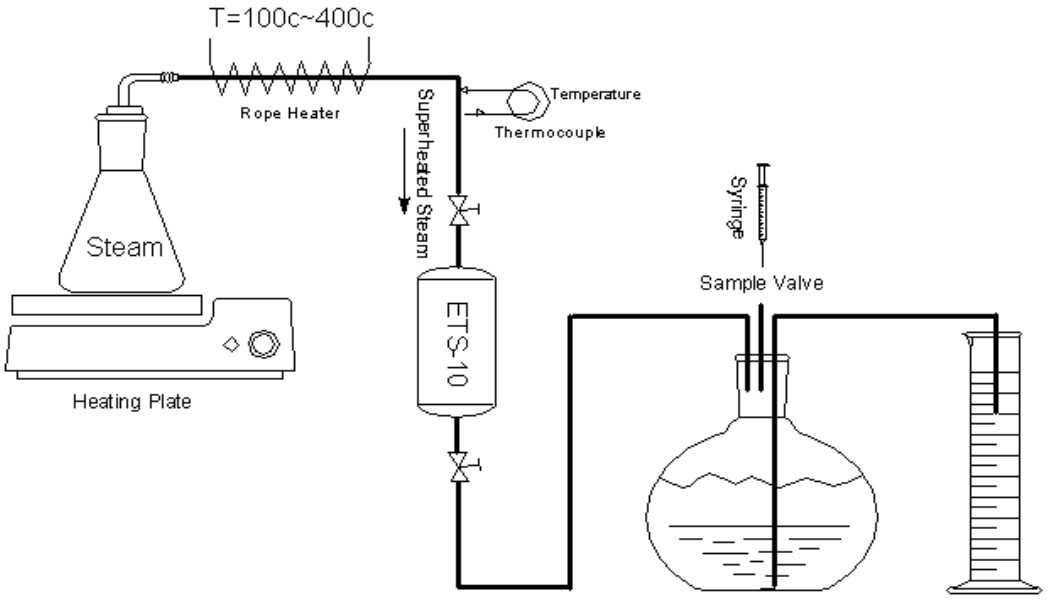

Figure 4-2 Experimental schematic of the steam desorption process

The volume of the water displaced was tracked with time and the gas was sampled and tested with GC.

When the chamber cools to room temperature, connect the chamber with the feed gas, and a check was done to see if the adsorbent could be used for the next cycle.

4.2.3 Microwave desorption

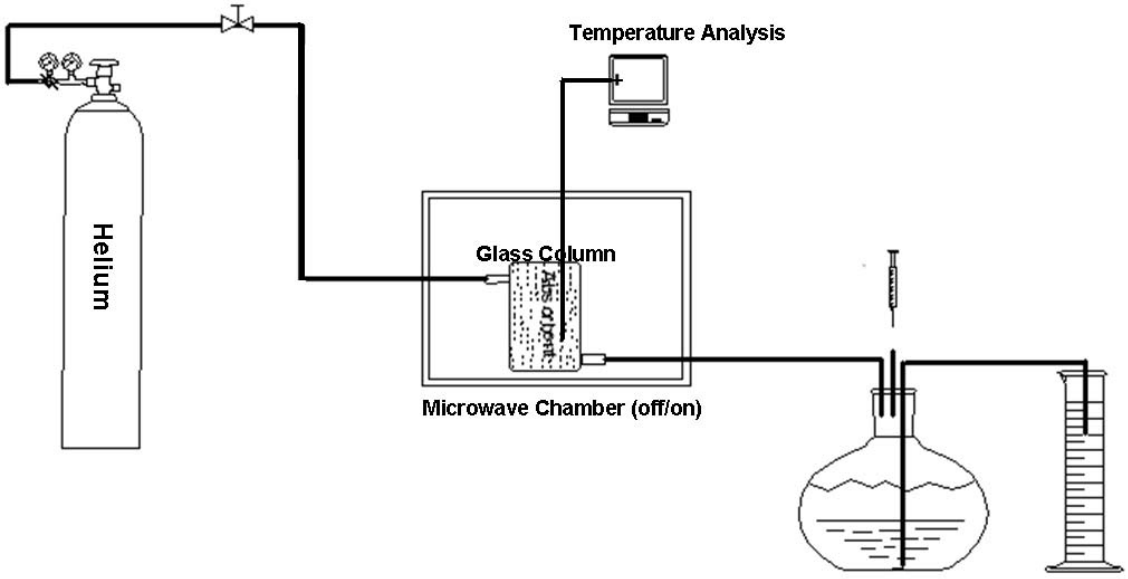

Figure 4-3 Experimental schematic of the microwave desorption process

Figure 4-3 illustrates the schematic of the microwave desorption process. The microwave was a modified kitchen microwave chamber. The temperature inside the glass column was tested and controlled by a Neoptix Reflex fiber optic temperature sensor. After the adsorption, we turned on the microwave and used the same collection mechanism as the steam desorption to collect the gas released from the glass container. After finishing desorption, the materials were cooled down to room temperature and we re-ran the adsorption and the microwave desorption as described above.

4.3 Results and discussion

Figure 4-4 shows the relation between desorbed gas volume and time for thermal desorption. Under 250°C, gas begins to release after 15 min, and takes 70 min to desorb most of the adsorbed gas. Under 300°C, it takes 30 min to finish the desorption process. The mixture is mostly ethylene, and due to the double bond of ethylene, the force between ethylene and Na-ETS-10 is very stable, this means more energy is required to finish this thermal desorption.

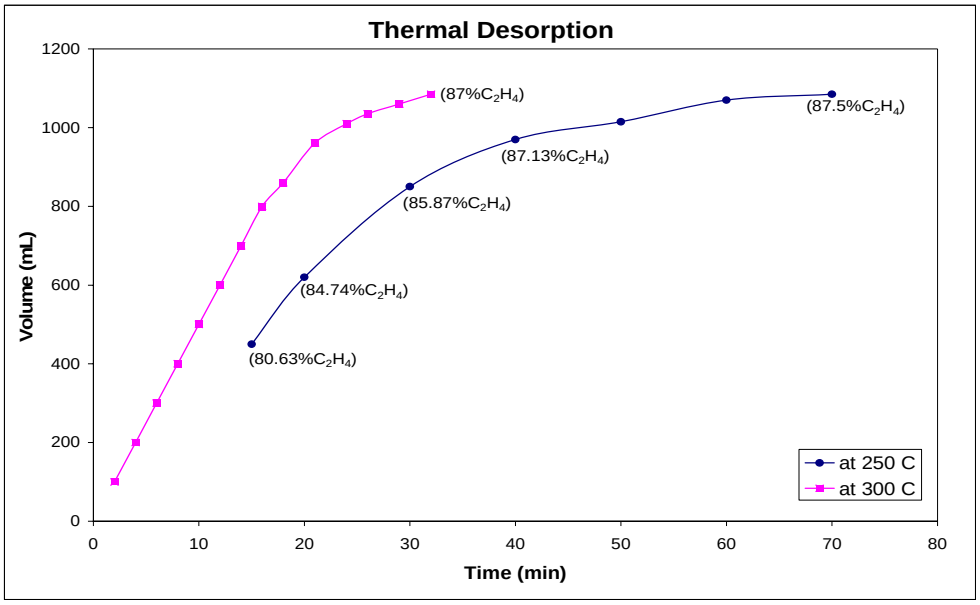

Figure 4-4 Volume of desorbed gas vs. time under thermal desorption

In our steam desorption experiment, as soon as we connected the steam with the double ended chamber, the gas came out and pushed the water out of the flask, and into the graduated cylinder. After 5 min no additional water came out which indicated that all the gas adsorbed by the adsorbent was replaced by steam. The volume of water pushed out by the gas was 1.2 L which reflects the volume of the adsorbed phase of the gas. The IGC

analysis result was 88% C_2H_4 and 12% C_2H_6, which matched the water desorption result very well, this means the gas was almost completely desorbed. The adsorbent could not be directly reused for the next cycle. The reason for the deactivation of the adsorbent is thought to be the poor volume control of steam used in this experiment. The amount of the water molecules introduced may have exceeded the maximum acceptance of Na-ETS-10. If we thermally re-activated the adsorbent for 10 h at 150°C to remove the adsorbed water prior to reuse, the performance of the Na-ETS-10 did not degrade following steam desorption.

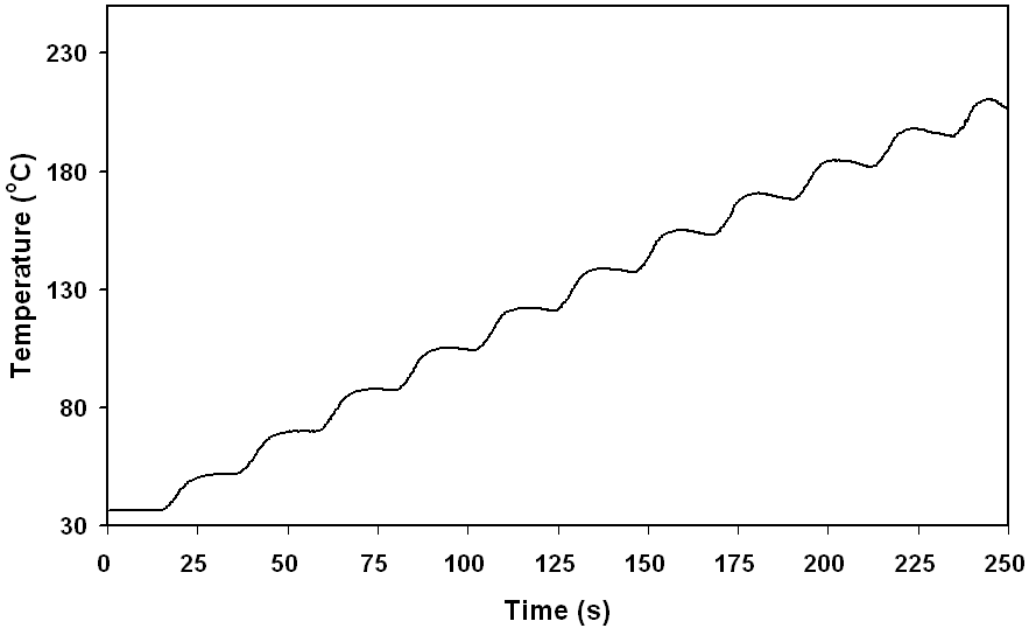

Figure 4-5 Temperature vs. time profile in a kitchen microwave oven

Microwave desorption was achieved by gradually increasing the temperature of the saturated Na-ETS-10 column (Figure 4-3) to 200°C, a temperature at which the Na-ETS-10 remained stable. The temperature increase inside the Na-ETS-10 column over the

course of a typical desorption experiment is shown in Figure 4-5. Under these heating conditions, 1.1 L of gas containing 86.89% C_2H_4 (IGC results shown in Figure 4-6) was collected in four minutes (6.1 bed volumes/min). This result was similar to those observed for steam desorption. The binary bed selectivity factor of Na-ETS-10 for ethylene over ethane under these conditions is 4.7. Further heating did not result in further hydrocarbon desorption. Following desorption, the adsorbent was allowed to cool to room temperature before the cycle was repeated. After a second adsorption/desorption cycle, 1.2 L of gas containing 87.1% C_2H_4 (IGC results shown in Figure 4-7) was collected in four minutes. Like steam desorption, microwave desorption did not degrade the performance of Na-ETS-10, however, microwave desorption is simpler and faster, as thermal re-activation of the sorbent is not required.

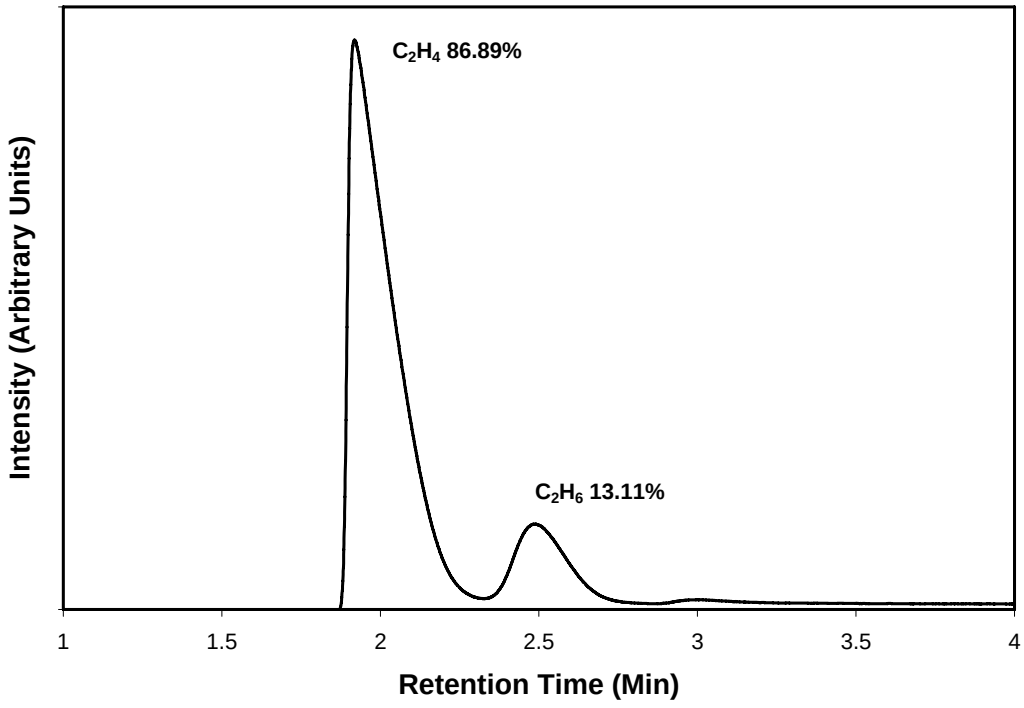

Figure 4-6 IGC analysis of the adsorbed phase gas in cycle one by microwave desorption

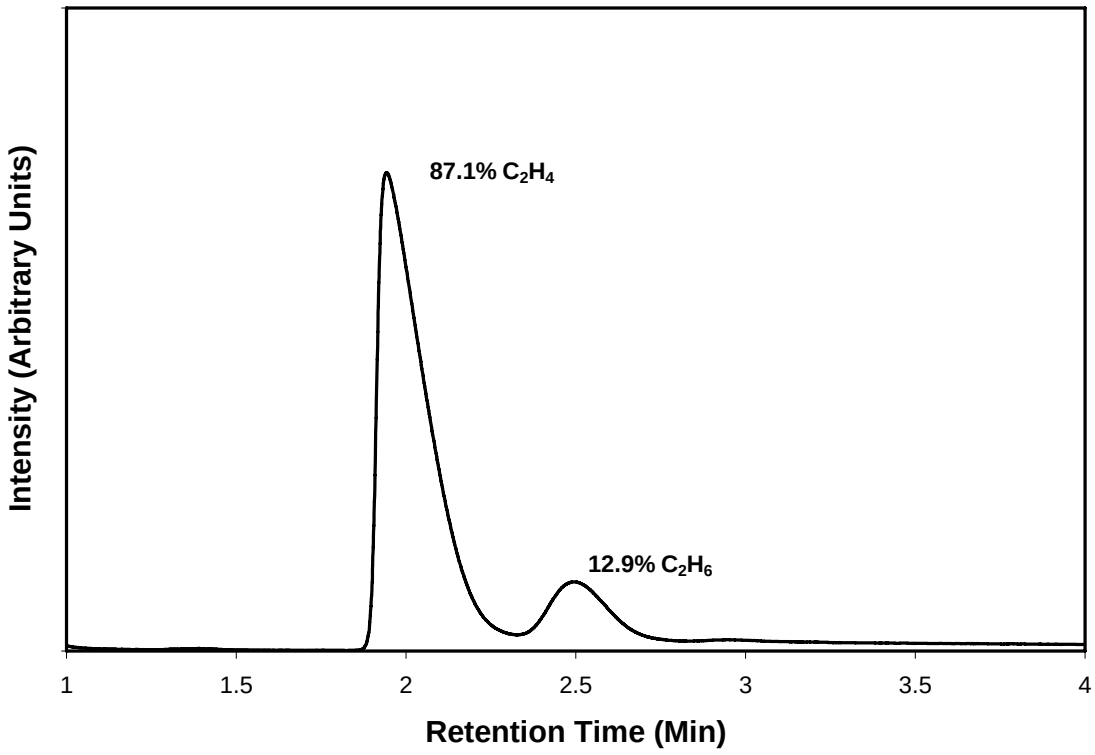

Figure 4-7 IGC analysis of the adsorbed phase gas in cycle two by microwave desorption

4.4 Conclusion

Thermal desorption is an energy intensive method for ethylene and ethane separation. Compared with microwave desorption, it takes 70 min to finish the process at 250°C, while microwaving only taking 4 min to finish the desorption. Microwave desorption is clearly a potential energy saving solution for the ethylene and ethane desorption process. The cycle tests prove that microwave can regenerate the adsorbent Na-ETS-10. Steam also shows its efficiency in desorption, but is complicated, requiring precise control over the amount of steam. Too much steam causes loss of capacity for the next run. Another possible solution is to use the microwave to generate the heat to activate the "wet" adsorbent used in the steam process. This could be tested in the future.

Chapter 5 Conclusion

We have demonstrated a physical separation of C_2H_4/ C_2H_6 using Na-ETS-10 by an equilibrium competitive adsorption mechanism. Under different binder system and flow rates, different mass transfer properties were observed. Using 15wt% Ludox as binder and 180 mL/min as the flow rate, from the flow-through experiment, we can get a stream of high purity ethane (100%) at the outlet of the unit which would allow ethane recycling for further cracking. We also obtain an enriched ethylene phase (~87%) upon desorption which could reduce energy costs in distillation units. Based on 30 g of Na-ETS-10, we can produce a 1.2 L mixture which contains 87% ethylene. This illustrates that, although we observe a selectivity of 12 under isotherm analysis and 12.59 under GC analysis for C_2H_4/C_2H_6 at ambient conditions, a binary bed selectivity of 4.65 can be obtained for ethylene/ethane.

Another adsorbent, Zn-RPZ, was tested for comparison. This selective adsorption separation is based on the steric effect. Using 30 g of Zn-RPZ, a 610 mL mixture containing 81.8% C_2H_4 and 18.2% C_2H_6 was obtained, which means we can get a binary bed selectivity of 3.12 for C_2H_4/C_2H_6 on Zn-RPZ.

The capacity and selectivity of Na-ETS-10 for ethylene increase at reduced temperature and elevated pressures that reflect the working conditions in ethylene plants. Under 8 atm and 0°C, we can produce 1584 mL of gas having a composition of 93% C_2H_4 by using approximately 30 g of Na-ETS-10. Under these conditions, the binary bed selectivity increases from 4.65 to 9.17.

Comparing thermal desorption, steam desorption, and microwave desorption, microwave is the most efficient for our ethylene and ethane separation unit. It can raise the

temperature to 200°C in 4 min and completely desorb all adsorbed phase gas. Regenerated adsorbent could be reused immediately and performed identically in a repeat cycle. This illustrated that microwave can efficiently regenerate and activate Na-ETS-10.

Our adsorption and microwave desorption processes are scalable, and represent a potentially cost-effective method for enriching ethane or ethylene. Further more assessment of energy efficiency should be done by the future work. The exact energy using in these three different desorption methods should be evaluated. Such as , how much heat was generated by the oven for thermal desorption, how much electricity was used to generated the steam, and how much electricity to supply for the microwave to complete the desorption. Especially when we talk about an industrial ethylene plant scale, whether microwave is still be able to be applied will be a question. After these comparison and evaluation, we can decide which method is doable in industry and which one is a real low cost and high efficiency desorption option.

Further work will be also needed to improve this method for ethane and ethylene separation. It may be possible to improve the adsorbent through ion exchange, and to improve the transfer properties of the adsorbent pellets through changes to the binder system. Significant thought and effort will need to be dedicated to the concept of process scale-up, in order to apply this separation in a real ethylene plant. These next steps will likely need to be informed by consultation with our industrial colleagues.

References

Al-Baghli, N.A., Loughlin, K.F., 2006. *Binary and ternary adsorption of methane, ethane, and ethylene on titanosilicate ETS-10 zeolite*. Journal of Chemical and Engineering Data 51, 248-254

Anderson, M.W., Terasaki, O., Ohsuna, T., Philippou, A., Mackay, S.P., Ferreira, A., Rocha, J., Lidin, S., 1994. *Structure of the microporous titanosilicate ETS-10*. Nature 367, 347-351

Ania, C.O., Menendes, J.A., Parra, J.B., Pis, J.J., 2004. *Microwave-induced regeneration of activated carbons polluted with phenol. Acomparison with conventional thermal regeneration*. Carbon 42, 1383-1387

Anson, A., Wang, Y., Lin, C.C.H., Kuznicki, T.M. and Kuznicki, S.M., 2008. *Adsorption of ethane and ethylene on modified ETS-10*. Chemical Engineering Science 63, 4171-4175

Bradshaw, S.M., VanWyk, E.J., De Swardt, J.B., 1998. *Microwave heating principles and the application to the regeneration of granular activated carbon.* Journal of the south African Institute of mining and metallurgy 98 (4), 201-210

Breck, D.W., 1974. *Zeolite Molecular Sieves*. Wiley: New York

Brunauer, S., 1943. *The Adsorption of Gases and Vapors Vol I-Physical Adsorption*. Princeton University Press

Burns, R.L., Koros, W.J., 2003. *Defining the challenges for C_3H_6/C_3H_8 separation using polymeric membranes*, Journal of Membrane Science 211, 299-309

Cha, C.Y., Carlisle, C.T., 2001. *Microwave process for volatile organic compound abatement.* Journal of the Air and Waste Management Association 51(12), 1628-1641

Chang, J.-W., Marrero, T.R., Yasuda, H.K., 2002. *Continuous process for propylene/propane separation by use of silver nitrate carrier and zirconia porous membrane*. Journal of Membrane Science 205, 91-102

Coss, P.M., Cha, C.Y., 2000. *Microwave regeneration of activated carbon used for removal of solvents from vented air.* Journal of the air and waste management association 50 (4), 529-535

Crønsted, A.F., 1756. Akad. Handl. Stockholm 18, 120

Eichorn, 1858. H., Ann. Physik. (Poggendorf) 105, 126

Flanigen, E.M., 1980. *Molecular sieve zeolite technology-The first twenty-five years.* Pure & Applied Chemistry 52, 2191-2211

Global Industry Analysts (GIA), 2008. *Ethylene: A Global Strategic Business Report*

Habgood, H.W., 1964. *Adsorption and gas chromatographic properties of various cationic forms of zeolite X*. Canadian Journal of chemistry 42, 2340-2350

Http://www.plastemart.com/upload/Literature/Ethylene-producers-Middle-East-advantages-low%20prices-economic-slowdown.asp

Inglis, R.S., Thomas, O., 1987. *Microwave regeneration of adsorbent materials for reuse as drying agents*. US Patent 4,805,317

Kniel, L., 1980. *Ethylene, keystone to the petrochemical industry.* Marcel Dekker, Inc. New York and Basel

Kong, Y. and Cha, C.Y., 1996. *Microwave-induced regeneration of NO_x-saturated char.* Energy & Fuels 10 (6), 1245-1249

Kong, Y., Cha, C.Y., 1995. *NO_x abatement with carbon adsorbents and microwave energy.* Energy & Fuels 9 (6), 331-337

Kuznicki, S.M., 1989. *Large-pored crystalline titanium molecular sieve zeolites.* US Patent No. 4,853,202

Kuznicki, S.M., 1990. *Preparation of small-pored crystalline titanium molecular sieve zeolites.* US Patent No. 4,938,939

Kuznicki, S.M., 1991. *Large-pored crystalline titanium molecular sieve zeolites.* US Patent No. 5,011,591

Kuznicki, S.M., Valerie, A., 2003. *Olefin Separations employing CTS molecular sieves.* US Patent No. 6,517,611

Kuznicki, S.M., Kelly, D.A., Bian, J., Lin, C.C.H., Liu, Y., Chen, J., Mitlin, D., and Xu, Z., 2007. *Metal nanodots formed and supported on chabazite and chabazite-like surfaces*. Microporous & Mesoporous Materials 103, 309-315

Kuznicki, S.M., 2008. *Titanium silicate materials, method for their manufacture, and method for using such titanium silicate materials for adsorptive fluid separations*. WIPO Patent Application WO/2008/002463

Kuznicki, S.M., Ansón, A., Segin, T., and Lin, C.C.H., 2009. *Modified ETS-10 zeolites for olefin separation.* U.S. Patent Application 20090187053

Meredith, R.J., 1998. Engineers' Handbook of Industrial Microwave Heating. Institution of Electrical Engineers, London

Mer'kov, A.N., 1973. Zapiski Vses Mineralog. Obshch., 54-62

Plank, C.J., Rosinski, E.J., Hawthorne, W.P., 1964. *Acidic crystalline aluminosilicates: new superactive, superselective cracking catalysts.* Industrial & Engineering Chemistry Product Research and Development 3(3), 165–169

Pozar, D.M., 1998. Microwave Engineering. John Wiley & Sons, New York

Price, D.W., Schmidt, P.S., 1997. *Microwave regeneration of adsorbents at low pressure: experimental kinetics studies.* The Journal of Microwave Power and Electromagnetic Energy 32 (3), 145-154

Reine, T.A., Eldridge, R.B., 2005. *Absorption equilibrium and kinetics for ethylene-ethane separation with a novel solvent.* Industrial & Engineering Chemistry Research 44, 7505-7510

Reub, J., Bathen, D., Schmidt-Traub, H., 2002. *Desorption by microwaves: mechanisms for multicomponenet mixtures.* Chemical Engineering and Technology 25 (4), 381-384

Reub, J., Bathen, D., Schmidt-Traub, H., Hoffmeister, M., Binder, A., 2001. *Multicomponent desorption of fixed bed adsorbers by microwaves.* Ceramic Transactions 111, 427-434

Schweiger, T.A.J., LeVan, M.D, 1993. *Steam regeneration of solvent adsorbents.* Industrial & Engineering Chemistry Research 32 (10), 2418-2429

Sircar, S., Myers, A. L., 2003. *Handbook of Zeolite Science and Technology (Gas Separation by Zeolites)*. Marcel Dekker Inc., New York

Teramoto, M., Shimizu, S., Matsuyama, H., Matsumiya, N., 2005. *Ethylene/ethane separation and concentration by hollow fiber facilitated transport membrane module with permeation of silver nitrate solution,* Separation & Purification Technology 44, 19-29

Triebe, R.W., Tezel, F.H., Khulbe, K.C., 1996. *Adsorption of methane, ethane and ethylene on molecular sieve zeolites*. Gas Separation & Purification 10 (1), 81-84

Vaughan, D.E.W., 1978. *Properties of natural zeolites. in natural zeolites: Occurrence, properties, use.* Pergamon Press: New York

Wu, Z., Han, S., Cho, S., Kim, J., Chue, K., Yang, R.T., 1997. *Modification of resin-type adsorbents for ethane/ethylene separation.* Industrial & Engineering Chemistry Research 36, 2749-2756

Yang, R.T., 1997. *Gas separation by adsorption processes*. Imperial College Press